Student thesis series INES nr 470

Vegetation phenology derived using the plant phenology index and the normalized difference vegetation index for the Balkan peninsula, south-eastern Europe

Aleksandra Ivanova

2019
Department of
Physical Geography and Ecosystem Science
Lund University
Sölvegatan 12
S-223 62 Lund
Sweden

Aleksandra Ivanova (2019).
Vegetation phenology derived using plant phenology index and normalized difference vegetation index for the Balkan peninsula, south-eastern Europe
Växtfenologi beräknad från satellitbaserade vegetationsindex för Balkanhalvön, sydöstra Europa.
Master degree thesis, 30 credits in *Geomatics*
Department of Physical Geography and Ecosystem Science, Lund University

Level: Master of Science (MSc)

Course duration: *August* 2017 until *January* 2018

Disclaimer

This document describes work undertaken as part of a program of study at the University of Lund. All views and opinions expressed herein remain the sole responsibility of the author, and do not necessarily represent those of the institute.

Vegetation phenology derived using plant phenology index and normalized difference vegetation index for the Balkan peninsula, south-eastern Europe

---

Aleksandra Ivanova

Master thesis, 30 credits, in *Geomatics*

Jonas Ardö
Lund University, Department of Physical Geography and Ecosystem Science

Lars Eklundh
Lund University, Department of Physical Geography and Ecosystem Science

Exam committee:
Hongxiao Jin,
Lund University, Department of Physical Geography and Ecosystem Science
David Tanenbaum,
Lund University, Department of Physical Geography and Ecosystem Science

ABSTRACT

Change in vegetation seasonality, associated with earlier start of plant activity in spring and longer length of the growing season, has been linked to global warming trends in recent decades. It is important to understand the spatiotemporal patterns of vegetation phenology change. Remote sensing observation techniques are broadly used in vegetation monitoring. Satellite phenology observations are based on spectral vegetation indices, yet vegetation phenology derived from satellite observations contain uncertainties. The overall goal of this study was to compare phenology metrics (start of season, end of season), estimated from two different vegetation indices- the commonly used Normalized Difference Vegetation Index (NDVI) and the recently developed Plant Phenology Index (PPI). Differences in spatial and temporal patterns in phenology metrics were investigated for part of the Balkan Peninsula region, South-eastern Europe for the period 2000 – 2016. Both indices were derived from MODIS Nadir BRDF satellite data and phenology metrics were estimated by applying a double-logistic function to PPI and NDVI time-series in TIMESAT program. In addition, a transect of sampling points was constructed within the study area, for further analysis. The relationships between the estimated phenology metrics and phenology driving factors (temperature, precipitation and altitude) were analysed. The results revealed that PPI and NDVI differ considerably in their phenology metrics estimates, with NDVI generally preceding PPI in the start of the season estimates and estimating later end of the season. PPI showed better correlation with the examined phenology driving factors and had reported better agreement with ground phenology observations in deciduous and coniferous forests. Phenology metrics trends were examined and showed an advancing trend for the beginning of the growing season in the spring and delaying trends for the end of season in the autumn.

TABLE OF CONTENTS

LIST OF ABBREVIATIONS

BAN	Bulgarian Academy of Science
BRDF	Bidirectional reflectance distribution function
CLC	Corine land cover
DOY	Day of year
EEA	European Environmental Agency
EMS	Electromagnetic spectrum
ENVI	ENvironment for Visualizing Images
EOS	End of season
ESA	European Space Agency
GPP	Gross Primary Production
HDF	Hierarchical Data Format
LAI	Leaf Area Index
LP DAAC	Land Processes Distributed Active Archive Center
LPS	Land surface phenology
MK	Mann-Kendall trend analysis
MODIS	Moderate-resolution Imaging Spectroradiometer
NASA	National Aeronautics and Space Administration
NDVI	Normalized Difference Vegetation Index
NIHM	National Institute of Meteorology and Hydrology
NIR	Near-infrared
PPI	Plant Phenology Index
SOS	Start of season
SRTM	Shuttle Radar Topography Mission
TS	Theil-Sen slope estimator
VI	Vegetation Index

1 INTRODUCTION

Phenology is the study of life-cycle events of organisms, and their responses to seasonal and inter-annual variation in climate (Morisette et al. 2009). Specifically, vegetation phenology focuses on plants life-cycles, as well on a understanding the underlying processes driving certain stages in their biological life. Historical phenology records of cherry flowering in Japan stretch back to the eight century and in Europe records dates back to the early 1700s (Sparks and Menzel 2002). Plant phenology is revealing to be a strong indicator of the seasonality of the environment (Sparks and Menzel 2002), since the relationship between plant phenology stages and temperature and precipitation has been proven in numerous studies (Menzel et al. 2006; Parmesan 2006; Cleland et al. 2007; Morisette et al. 2009; Wang et al. 2016). Furthermore, this climate to ecosystem relationship functions in both directions, with plants providing feedback to the climate system, as well (Parmesan 2006; Kueppers et al. 2007). The plant phenology inter-annual dynamics regulate ecosystem services, such as water balance, carbon and energy exchange between the ecosystems and the atmosphere (Richardson et al. 2013). Changes in seasonality, associated with an earlier start of plant activity in spring and longer length of the growing season, have been linked to the global warming trends in recent decades (Keatley and Hudson 2010). Therefore, plant phenology could be used as an indicator of climate impacts on terrestrial ecosystems at different spatial and temporal scales and should be incorporated in future climate modeling (Schwartz 2013).

Remote sensing observation techniques are broadly used in vegetation monitoring. Satellites are designed to monitor the Earth surface from space continuously, providing a different perspective from ground phenological records, which focus mostly on specific plant species and cover discrete areas. Capturing general plant canopy characteristics is fairly complicated, since there is considerable variability in seasonality among different plant species (Studer et al. 2007; Morisette et al. 2009). Earth observing satellites are carrying sensors, called imaging spectrometers, which use the sun light energy reflected by plants (spectral reflectance) to measure vegetation cover and its physical state (Graham 2012). Spectral remote sensing senses electromagnetic radiation and it measures how it is interacting with objects on the Earth surface. Plant canopies interact with sun radiation in three ways. It can be either transmitted (go through the canopy), absorbed by the canopy (use the energy to drive photosynthesis) or reflected off it (Graham 2012). Spectral remote sensing measures the reflected radiation in a way that the objects with higher reflectance appear brighter on the

satellite images. Plants reflect energy in different wavelengths; some are part of the visible range of the electromagnetic spectrum (EMS) and some are out of this range, not visible for the human eye. Plants spectral reflectance characteristics are determined by the physical structure and chemical composition of their leaves (Graham 2012).

Plant phenology derived using remote sensing is defined as land surface phenology (LSP) (de Beurs and Henebry 2004). LSP uses satellite-based observations to consistently generate estimates of the phenology phases (start, peak, duration, and end of the season) of green vegetation (Reed et al. 2009). Existing research on LSP is often based on spectral vegetation indices (VI). VIs are usually dimensionless measures derived from mathematical combinations and transformations of the amounts of spectral reflectance of vegetation (Graham 2012). Most VIs are based on the reflectance measured in the visible and near-infrared regions (NIR) of the EMS, where high reflectance occurs.A common VI is the Normalized Difference Vegetation Index (NDVI). This index is calculated from reflectance in the red and NIR regions. It has been used since 1970s (Rouse et al. 1973) and has been proven to be a useful indicator of green vegetated areas. It is considered one of the traditional VIs and throughout its relatively long history of use in practise and studies, many of NDVI's limitations were revealed. To avoid some of those limitations, a physically-based Plant Phenology Index (PPI) was recently developed (Jin and Eklundh 2014).

1.1 Problem statement

Plant phenology derived from satellite VIs contains uncertainties, resulting in biased LSP estimates. NDVI encounters problems related to saturating the signal at high biomass levels (Huete et al. 2014); depicting the seasonality in greenness signal for evergreen vegetation, which has a relatively low inter-annual variability in photosynthetic activity (Reed et al. 2009); and sensitivity to snow, resulting in NDVI-based phenology coinciding with snow seasonality better than with actual plant phenology (White et al. 1997; Delbart et al. 2005; Jin et al. 2017). PPI was designed to overcome some of those challenges. It has been proven to surpass NDVI in estimating LSP for areas with seasonal snow cover and dominated by dense coniferous forests (Jin and Eklundh 2014; Jin et al. 2017; Karkauskaite et al. 2017).

In this work, a comparison between PPI and NDVI derived phenology metrics – such as the start of season and end of season, has been conducted for the period 2000 to 2016 for ecosystems on the Balkan Peninsula, South-Eastern Europe. To date, PPI and NDVI

comparisons have been applied in studies mostly focusing on the Boreal ecosystems in the Northern Hemisphere (Jin and Eklundh 2014; Jin 2015; Karkauskaite et al. 2017). PPI and NDVI phenology metrics would be compared against ground phenology observations for selected representative tree species for both forest types.

Phenology metrics have been used as a proxy for reconstructing past climate conditions and model future climate change (Beniston 2015). In the context of climate change, it is important to understand how climate factors influence vegetation seasonality. In this study the relationship between phenology, temperature, precipitation is analysed, in order to examine which is the dominant climate factor. Additionally, remotely sensed data is used to identify which phenological metrics variations could be explained by altitude gradient as a factor.

1.2 Research objectives

The overall goal of this study is to compare phenology metrics, estimated from two different VIs –PPI and NDVI, derived from MODIS satellite data, to investigate trends in spatial and temporal patterns of phenology in the Balkan Peninsula region.

The main objectives to achieve this goal are the following:

1. Identify if the derived phenology metrics significantly differ between PPI and NDVI.
2. Investigate the spatial patterns of PPI and NDVI phenology.
3. Examine the relationships between PPI and NDVI phenology and climate factors (temperature, precipitation) and altitude along a transect.
4. Examine the trends in PPI and NDVI phenology for different land cover types and along a transect within the study area.
5. Compare PPI and NDVI phenology metrics with ground phenology observations for broad-leaved and coniferous forest types.

2 BACKGROUND

2.1 Phenology

Phenology was defined by Leith (1974) as the study of the timing of recurring biological events, the causes of their timing with regard to biotic and abiotic forces. First budburst, canopy growth, flowering, leaf unfolding, leaf fall are all examples of the life-cycle biological events of vegetation. Plant phenology has been used to observe climate and weather patterns throughout human history. For a long time, phenology studies have been closely related to agriculture, and its applications were limited to inventories, focusing on specific plant species and mostly on the local level. In the last few decades, the view of the scientific community towards the field of phenology has changed. Phenology has been recognized as an environmental science with the potential for addressing a variety of ecosystem problems (Schwartz 2003). This shift was primary driven by the establishment of continuous observation networks in the 1990s, investigating species behavior and how it changes due to environmental factors. The publications of early researchers have proven the potential which phenology analysis can provide for better understanding of climate change's impacts on ecosystems (Schwartz 2013). With the trend of continuous global warming, the interest in phenological research and applications has been growing (Keatley and Hudson 2010). The interdisciplinary nature of Phenology is highlighted in the book "Phenology: An Interactive Environmental Science" by Schwartz, which compiles a detailed overview on: phenological data, networks, research, applications, remote sensing phenology in different continents and in selected bioclimatic zones. It also discusses the current state of the field methodology limitations and future prospects in the phenology research.

Many European countries have a long tradition in systematic observations and collection of phenological data. Those records are a suitable foundation for investigating phenology changes at the continental scale or providing reliable validation ground truth data for satellite phenology data. In practice, in different countries plant phenology observations and data collection evolved in different traditions (taxa differences, measuring techniques, sample methods, quality control, observed species etc.). Compiling and facilitating standardized and homogenous plant phenology data sets, which can provide a complete overview at continental level, is still challenging. However, in the last decade phenology data was incorporated in to research on global change. International efforts on harmonizing ground

phenology observations, from different locations across Europe, have been made. Initiatives, promoting phenological research, such as The International Phenological Gardens (IPG) of Europe was founded in 1957, COST Action725 was established 1971, and its successor PEP725 European phenological database, have the purpose of delivering a pan european phenological database with identical standards, plant species, definitions on terminology and guaranteeing the production of high quality data (Sparks and Menzel 2002). However, international phenology networks are concentrated in West, Central and North Europe and do not include all the different ecological and climate regions of the continent. Greater Collaboration between European countries is still needed (Schwartz 2013).

2.2 Remote sensing phenology

In the past few decades, satellite-based observations have been recognized as an essential tool in plant phenology retrieval. Sensors mounted on satellites orbiting the Earth deliver data with high spatial and temporal resolution. While ground observations would be limited to representing local conditions, spectral remote sensing has the capabilities to capture changes in vegetation properties at a different extents – from local to continental and global (Zhang et al. 2012).

As mentioned above, spectral remote sensing measures how electromagnetic radiation interacts with the plant canopy. Typically plant leaves absorb light in the red and blue visible regions of EMS, to use in the photosynthesis processes; light is reflected in some parts of the green region, therefore plants appear green to human eye; and even stronger reflectance occurs in the NIR, out of the visible part of the EMS (Gates et al. 1965).With seasonal changes in the plant canopy from spring to autumn, these reflectance properties also change.

The interaction with the canopy is not only dependent on the wavelength. Spectral reflectance and spectral absorption magnitudes are based around several characteristics of vegetation (Graham 2012). Structural properties of individual leaf, such as cell structure, thickness, age, pigmentation and water content, are reflected in different parts of the of the EMS (Xue and Su 2017). High absorption of energy is targeted around the visible red band (620 - 700 nm) and it is related to chlorophyll content in the outer layers of the leaf; similarly absorbed is the energy from the blue band (450 – 490 nm), thus the majority of reflected energy has been found the green region (490 – 570 nm) of EMS; energy from the NIR region (above 700 nm) is not used in photosynthesis, thus plants reflect a large proportion of the NIR radiation

(Gates et al. 1965). These radiative properties of individual plants allow the distinguishing of different species on the basis of reflected radiation. However, remote sensing LSP observations are fundamentally different from ground observations, because of the limited capacity of satellite sensors to detect individual plant radiative dynamics from space due to resolution issues (Henebry and de Beurs 2013). The signal, represented on the satellite image pixel, is influenced by the soil (brightness, color, water content), the other vegetation present in the area of interest (mixed signal, water vapor, canopy shadow), and the atmosphere (atmospheric aerosols, cloud coverage) (Reed et al. 2009).

2.2.1 Vegetation Indices

2.2.1.1 NDVI

NDVI is the ratio of the difference between the near-infrared band (NIR) and the red band (RED), and the sum of these two bands (Rouse Jr et al. 1974):

$$NDVI = \frac{NIR - RED}{NIR + RED}, \tag{1}$$

The NDVI algorithm takes advantage of the fact that green vegetation reflects less visible light and more NIR, while sparse or less green vegetation reflects a greater portion of the visible and less NIR. NDVI combines these reflectance characteristics in a ratio, so the range of values obtained is between −1 and +1. It is assumed, that only positive values correspond to vegetated zones; the higher the index, the greater the chlorophyll content of the targeted plant canopy.

NDVI is applied in the assessment of general amount of vegetation, canopy structure, calculating leaf area index (LAI), indicating gross primary production (GPP) and other plant canopy characteristics (Gitelson 2004; Xue and Su 2017). However, studies based on NDVI revealed that the existing methods for retrieval of LSP often involve uncertainties. NDVI happened to be less sensitive to the dynamics of photosynthetic activity in densely vegetated areas (Sellers 1985; van Wijk and Williams 2005; Glenn et al. 2008). Thus, NDVI estimates of LAI and other biophysical characteristics should be treated with consideration of those

limitations. This is especially true for ecosystems dominated by evergreen vegetation (Delbart et al. 2005; White et al. 2009).

2.2.1.2 PPI

PPI is a physically-based spectral index for retrieving plant phenology and is formulated to have a nearly linear relationship to green LAI, given a fixed soil effect (Jin and Eklundh 2014). PPI is formulated based off a modified version of Beer's law, which describes the relationship between canopy reflectance and LAI, and it is in the same unit (m^2 m^{-2}). PPI is calculated as follows:

$$PPI = -\mathrm{K} \times \ln \frac{(\mathrm{NIR} - \mathrm{red})_{max} - (\mathrm{NIR} - \mathrm{red})}{(NIR - red)_{max} - (NIR - red)_{Soil}}, \quad (2)$$

where *NIR* and *red* are nadir-viewing reflectance in NIR and red range of EMS. *K* is the gain factor that is formed as a function of sun zenith angle θ, a geometric function of leaf angular distribution and instantaneous diffuse fraction of solar radiation. *K* is formulated as:

$$K = \frac{0.25 \cos(\theta)}{(1 - \mathrm{d}_c)G + \mathrm{d}_c \cos(\theta)} \frac{1 + (NIR - red)_{max}}{1 - (NIR - red)_{max}}, \quad (3)$$

where θ is the sun zenith angle; d_c is an instantaneous diffuse fraction of solar radiation for clear sky and standard atmosphere, when the sun is at zenith angle θ; *G* is a geometric function of leaf angular distribution fixed to value of 0.5 for either flat or needle leaf.

For complete details on the formulation of the Plant Phenology Index, see Jin and Eklundh (2014). They also demonstrate the PPI-LAI relationship through satellite derived PPI and field LAI data; PPI robustness against snow influence; and noise during the phenology transition period, showing improved performance over NDVI for indicating vegetation fundamental properties.

3 MATERIAL AND METHODS

3.1 Study area

3.1.1 Location

In the first stage of the project, the study was focused on MODIS tile - h19 v04 (Figure 1). The tile covers most of the Balkan Peninsula, located in South-eastern Europe, excluding central and south Greece and the west coast of the Black sea. In the second stage, a transect within the study area was defined, located in Bulgaria. The transect path includes a representative variety of European land covers, regarding vegetation and environmental conditions, although those dominant ecosystems are presented in other European countries with considerably larger territories (Yurukov and Zhelev 2001). The transect spans in a north-south direction (Figure 2), composed of 342 sampling points placed along a linear feature, with a distance of 463 meters in between points. The starting point is located at 42°59'14.035"N latitude and 24°58'26.861"E longitude and the ending point is located at 41°35'1.747"N latitude and 24°42'21.896"E longitude. Transect altitude ranges between 153 and 2376 meters and stretching along complex relief. The transect perpendicularly crosses the main range of Stara Planina Mountains, through its highest peak (Botev, 2376 m), including typical temperate, sub-alpine and alpine ecosystems. In the southern direction, the Thracian Plain is located, mostly occupied by cultivated lands with a reduced presence of natural vegetation. Subsequently, this is followed by the Rhodope mountain range, dominated by natural deciduous and coniferous forests (Bondev 1991).

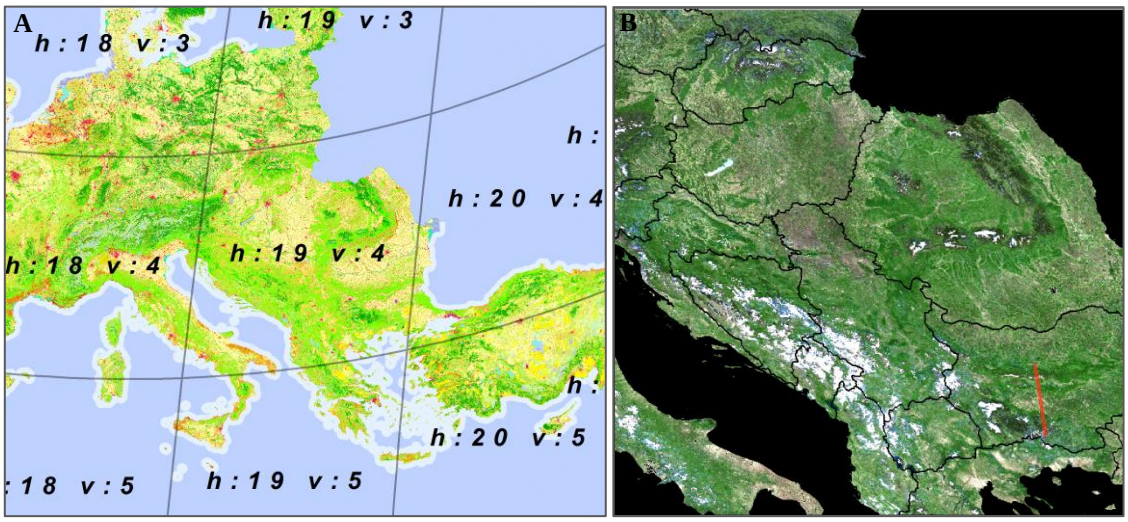

Figure 1. A) MODIS tiles boundaries over CORINE land cover ; B) MODIS tile h19v04 true colour composite with the transect (red line)

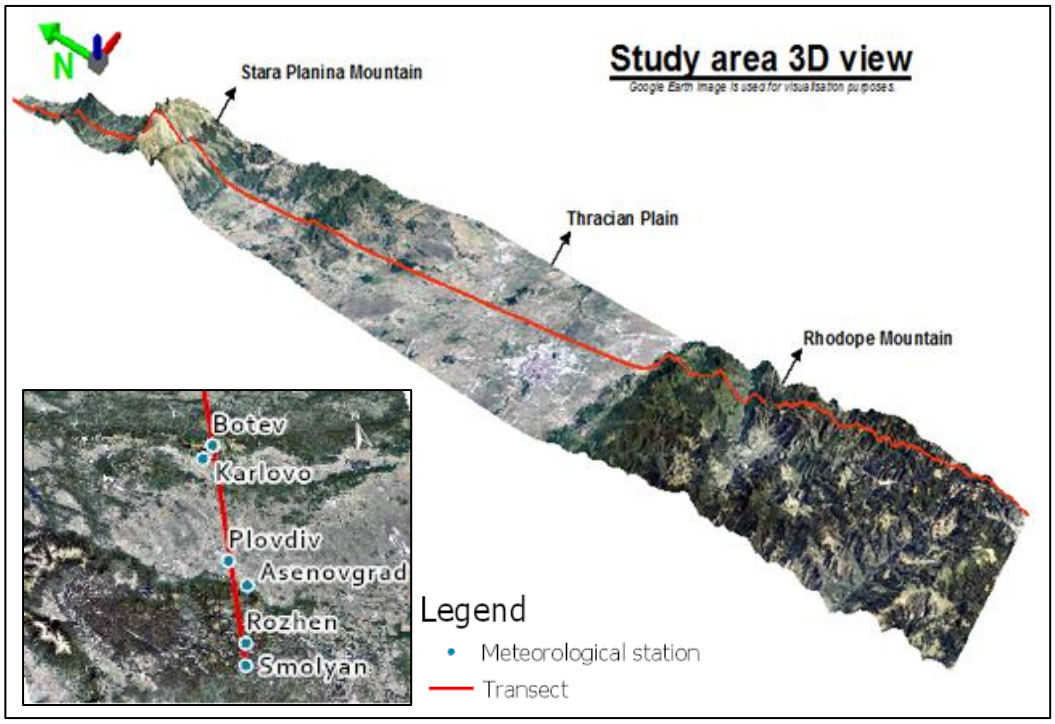

Figure 2 Study area transect in Bulgaria, consisting of 342 points along around 160km distance (red line) and the six meteorology stations over Google Earth image.

3.1.2 Climate and seasonality

This territory is situated in the transition zone between the continental climate and the sub-Mediterranean climate (Kottek et al. 2006). The mean annual temperatue vary from 3.0 Cº to 14.0 Cº depending on location and elevation. The mean monthly temperature in the area in January varies from -11.0 Cº to 3.0 Cº and from 5.0 Cº to 25.0 Cº in July. Mean annual precipitation in the Rhodope mountains are between 700 – 1100 mm (Letchov 2012). Study conducted by Brwon and Petkova (2007), analyses snow cover variability in Bulgaria for the period 1931 – 2000. They reported that stable snow cover appears in the area in the end of December and disappearing gradually between the end of February (below 800 m) and the beginning of April (above 1600 m). There is a trend of shortening of the snow cover season, which is driven by later snow cover onset and reduced winter precipitation. It has to be noted, there is no trend reported towards earlier beginning of the spring thawing period, as in other parts in Europe. Phenology as an indicator climate conditions is studied in the area of interest by Prof. Kazandziev (Kazandjiev 2014), the paper summarizes how climate change affects the vegetation development in Bulgaria. Steady transition of daily average temperature across

5 Cº was taken for starting date of the spring vegetative season, which is in the beginning of March for the lowlands and beginning of April for the mountains. Despite the significant spatial variability there is a consistent signal of earlier start of the growing season. Fall pheno phases are later in the year, which is related to increase in fall temperatures and later snow cover. Recent studies in the area revealed an opposite trend of delay in SOS for some areas and discrete species in the region, it has to be noted the results depend on the length of the time period chosen for the study (Letchov 2012).

3.2 Data

3.2.1 PPI data

PPI data was provided from The Department of Physical Geography and Ecosystem Science, Lund University and it is available at ftp://pheno.nateko.lu.se/PPI_2000_2017/Tiles/h19v04/. PPI data was derived from MODIS satellite data and was organized as MODIS data and obtained for tile h19 v04 over the period 2000 to 2016.

3.2.2 Satellite data

Satellite data were obtained from https://lpdaac.usgs.gov/ maintained by the NASA Land Processes Distributed Active Archive Center (LP DAAC). Moderate-resolution Imaging Spectroradiometer (MODIS) multi-spectral sensors are designed to monitor Earth's atmosphere, ocean and land surface, and the instruments are mounted on board of Terra and Aqua satellites, launched by NASA launched in 1999 and 2002, respectively. MODIS sensors capture data in 36 spectral bands with a swath width of 2300 km, resulting in the production of various geophysical data products.

The MODIS Nadir bidirectional reflectance distribution function (BRDF)—Adjusted Reflectance product (MCD43A4, collection 5) was used for calculating NDVI. MODIS Nadir BRDF reflectance data is corrected to model the values as if they were taken from nadir viewing geometry (Schaaf et al. 2002). The MODIS product provides multi-date, multi-spectral, cloud-cleared, atmospherically corrected surface reflectance images with 500-meter resolution organized in a Sinusoidal grid system. Both Terra and Aqua satellites were used in generating the MCD43A4 product, temporally complementing each other, producing an image every 8 days with acquisition phase of 16 days. The MODIS Nadir BRDF product,

with red and NIR reflectance corrected for sun-sensor geometry, is particularly applicable for calculating a non-ratio based vegetation spectral index, such as PPI (Jin and Eklundh 2014).

3.2.3 Digital Elevation Model

The digital elevation model (DEM) used in this thesis is distributed by LP DAAC at http://dds.cr.usgs.gov/srtm/. The Shuttle Radar Topography Mission (SRTM) used a radar interferometry technique to develop the first global surface elevation data set collected using a consistent remote sensing method. Elevation is calculated by evaluating two different signals generated from two radar antennas (SIR-C and X-SAR). For the region of interest SRTM data is available as a 3-arc second (around 90m) resolution DEM. The original SRTM data collection was additionally processed to address areas with missing data, by applying interpolation techniques in combination with supplementary elevation data sources, resulting in the SRTM Void Filled product. All SRTM products are projected in the WGS84 horizontal datum and the EGM96 vertical datum (Farr et al. 2007). For the needs of this study, two SRTM Void Filled 3-arc second tiles were obtained (n41e024, n42e024), in GeoTIFF file format.

3.2.4 Land cover data

The CORINE Land Cover (CO-ordination of INformation on the Environment, CLC) is referring to a European inventory program that was initiated in 1985. The information is regularly updated (2000, 2006, 2012) by the European Environmental Agency (EEA), in cooperation with the European Space Agency (ESA), the European Commission, and its member countries. It has been derived from high-resolution satellite data (SPOT-HRV, Landsat-TM), photo-interpretation and validated by ancillary (in-situ) data: national orthophotos, topographic maps etc. The result is the CORINE database and cartographic product which consists of 5 main land cover groups, subdivided into 15 sections, which include 44 classes (European Environmental Agency 1994). CLC uses a minimum mapping unit of 25 hectares for areal phenomena and a minimum width of 100 m for linear phenomena. In this work, the latest version of CLC from 2012 is adopted to evaluate how phenology metrics vary spatially across different land cover classes. The whole data set is available for download from the Copernicus program web page at http://land.copernicus.eu .

3.2.5 Climate data

The climate data set used in this thesis is produced and provided by National Institute of Meteorology and Hydrology, Bulgarian Academy of Science (NIHM-BAN), and it is available upon request on http://www.meteo.bg/en. Temperature and precipitation data is acquired from six meteorological stations – Botev, Karlovo, Plovdiv, Asenovgrad, Rozhen and Smolyan, part of the bulgarian national meteorological network (Appendix, Table A1).

3.2.6 Phenology data

The ground phenology data set used in this thesis was also produced and provided by NIHM-BAN. Phenological data is distributed by the Department of Climatology and Agrometeorology, NIHM-BAN after official request at http://agro.meteo.bg/en. Four of the meteorological stations conduct phenological observations - Karlovo, Plovdiv, Asenovgrad, Smolyan. Four representative tree species were selected to assess the performance of satellite-based phenology metrics to ground observations. The ground phenology data set is described in Appendix Tables A2. Observation dates were collected for five phenological phases of coniferous species - first buds, buds bursting, needle, needle colouring and needle fall (Tables A3, A4 and A5) and eight phenological phases for broadleaved species - first buds, buds bursting, leaves unfolding, flowering, fruits, fruits fall, leaves colouring and leaves fall (Table A6). Observation sites were not provided with their exact coordinates. Instead they were described by the name of the phenological station.

3.3 Data pre-processing

3.3.1 Raster data

MODIS tile h19v04 observation images were downloaded for every 8 days (46 observations per year) for the period 2000 to 2016. Each MODIS tile is 10 by 10 degrees in size (2400 columns x 2400 rows, 463 x 463 m pixel size) and is projected in the Sinusoidal projection. NDVI was calculated for each satellite scene, following the steps of PPI data processing documented in a report provided with the data (Ardö 2017). The spectral bands used for calculation of the NDVI include band 1 (620-670 nm) and band 2 (841-876 nm), corresponding to the red and NIR ranges of the EMS, respectively. The native format of the MODIS data is Hierarchical Data Format (HDF), all images were converted to ENVI format, raw flat-binary image file with a separate header file (.hdr). Due to atmospheric corrections

and snow masks, information in the images is missing, often in the mountain regions and in images capturing winter seasons, which influences VIs calculation. Since the Terra satellite was launched in December 1999, the first image acquisition date of MCD43A4 product for tile h19v04 is 18th of February, corresponding to Julian day 049.The first six observation images for the year 2000 are missing – 001, 009, 017, 025, 033 and 041 (Julian day). This gap of missing data was filled using the arithmetic mean values of the VI images for years 2001-2003 originating from the same Julian day ($VI_{2000} = \frac{VI_{2001}+VI_{2002}+VI_{2003}}{3}$). Data for the surrounding years of period 2000-2016 is included, as suggested by Jönsson and Eklundh (2004), to reduce the risk of errors in the season determinations for the first and last years in the time-series. Dummy data was created for the year 1999 (identical to year 2000) and for the year 2017 (identical to year 2016).

All raster data sets were integrated in a database, following the MODIS data set format. SRTM and CLC data set were reprojected to the global Sinusoidal projection used by MODIS products and resampled to the 463 x 463 m pixel size; the harmonized data set allows further analysis to be carried out.

3.3.2 Time-series seasonality fit

MODIS data tends to be noisy, therefore it is difficult to estimate phenology parameters directly from the satellite images (Tan et al. 2011). Additionally, different vegetation types exhibit different inter-annual variations in their phenological phases, because of the complex composition of plant species, soil types, climate regimes and land cover management.

TIMESAT is a program developed by Jönson and Eklundh (2004) for processing time-series of satellite sensor data and extracting seasonality parameters and it is available at http://web.nateko.lu.se/timesat/timesat.asp. The TIMESAT software package was chosen to derive phenology metrics, because of the programs flexibility on gap-filling of noisy data and smoothing techniques for addressing diverse LSP patterns.

TIMESAT uses three fitting methods based on least-square fits to the upper envelope of the raw data, to take in to account that the most noise in VIs is negatively biased.The first one is an adaptive Savitzky–Golay filter. It uses local polynomial functions in the fitting, where defined moving window averages and replaces the raw values. The size of the moving window is too big, this could affect the ability to capture a rapid change in the time-series. On

the other hand, the small window fits close to the raw data, hence relatively clean data should be used. The other two filtering methods use a least-squared procedure to find the best-fit; they are Asymmetric Gaussians and double logistic functions. Both functions are based on intervals between minimum and maximum VI values in the time series, thus the methods are less sensitive to noise. The double logistic method has been reported to perform slightly better than the Gaussian function (Beck et al. 2006). It has been suggested that it is most suitable for describing vegetation dynamics in biomes with short seasonality or rapid transition between phenological phases, such as in Boreal and Alpine ecosystems (Beck et al. 2006; Jin et al. 2017). Therefore, the double logistic function was chosen to fit a smooth annual curve to the VI time-series in this work.

The double logistic function models VI data as a function of time using 6 parameters: minimum VI, maximum VI, two inflection points and two parameters related to the rate of change at the inflection points. The last two parameters are fixed in a range in TIMESAT to ensure smooth curve. To eliminate outliers and spikes from the VI time-series, a median filter was applied Values are defined as outliers in a moving window- if the value is larger than the maximum deviation it was set to the default value of two standard deviations.

3.3.3 Selection of phenology metrics

TIMESAT provides four methods for estimating start and end of season: seasonal amplitude, absolute value, relative amplitude and the Seasonal and Trend decomposition using Loess (Jönsson and Eklundh 2004). The third method takes into account the relative amplitude for the whole time-series, calculated as a difference between the mean maximum and the mean base level of the values. Start and end of season occur when a user specified fraction of this amplitude curve has been reached. After visually assessing test sites with different local conditions (forests, agricultural lands) and empirically controlling the amplitude parameters in relation with the STL trend, season start and ending amplitude fraction values were set to 0.2 for PPI time-series and to 0.4 for NDVI time-series. TIMESAT settings are displayed in Figure 3; it was assumed that NDVI time-series are negatively biased and values lower than zero do not represent vegetation, hence they were excluded from the seasonality fitting.

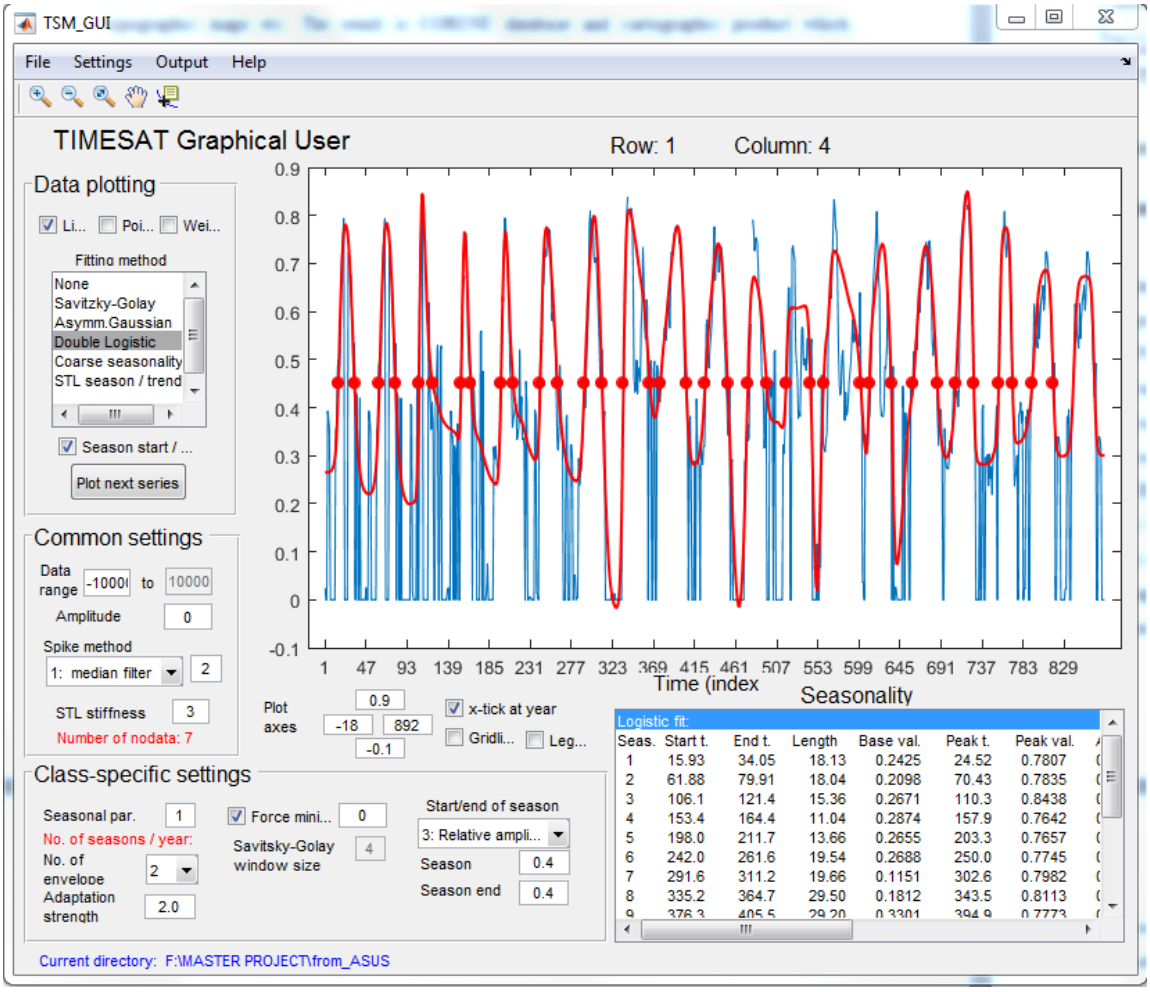

Figure 3. TIMESAT interface visualize settings to retrieve phenology metrics from NDVI time-series.

3.3.4 Climate data processing

Mean monthly temperature and precipitation was calculated for each year (2006-2015). Consequently, the monthly climate data was interpolated in a GIS environment to match the spatial extent of the study area, bounding the transect location. The inverse distance weighting interpolation method was chosen since the sample size is too small (6 stations) for applying more sophisticated interpolation techniques. Raster images with interpolated mean monthly temperature and precipitation values were produced for each month for the years between 2006 and 2015. Lastly, mean monthly temperature and precipitation values, over 10 years of observations, were calculated for each transects point.

3.3.5 Ground phenology data processing

Ground phenology data observations dates were averaged according to phenological phase (growing stages). Observation dates for "First budburst" and "Leaf unfolding" stages were selected to correspond to start of growing season retrieved from satellite-based phenology metrics. "Leaf coloring" and "Leaf fall" stages were chosen to be compared with end of season dates derived from PPI and NDVI phenology. Ground phenology observations data were available only for oak (Quercus spp.) and for one site (Smolyan station) for 3 years. Ground data was provided for three dominant coniferous tree species- spruce (Picea spp.), pine (Pinus spp.) and fir (Abies spp.), with better spatial and temporal quality. "Leaf coloring" and "Leaf fall" stages can be observed only for broadleaved tree species. Therefore, the growing stage of coniferous species associated with EOS was selected to be the date of autumn "Seeds fall" stage.

3.4 Statistical analysis

3.4.1 Analysis of phenology metrics response to climate factors

The annual timing in phenology phases is responding to air temperature and precipitation. The relationship between averaged monthly climate factors was established by applying a regression and assessed by the goodness of fit of the regression line, addressed by its coefficient of determination (r^2).

3.4.2 Phenology metrics trend analysis

To analyse phenology metrics trends and estimate their slopes, non-parametric methods were used - the Theil-Sen (TS) slope estimator (Theil 1950; Sen 1968) and the Mann-Kendall (MK) trend analysis (B. Mann and R. Whitney 1946). Non-parametric statistical tests do not assume a normal distribution of the data and are less sensitive to outliers, which makes TS and MK particularly suitable for noisy and short time-series (Jin 2015).

The Theil-Sen slope β describes the median slope between all $n(n-1)/2$ paired combinations over the time period as:

$$\beta = \underset{t2>t1}{^{median}} [(y_{t2} - y_{t1})/(x_{t2} - x_{t1})], \quad (4)$$

The trend is expressed as a rate of change in NDVI and PPI DOY per unit time.

The significance of the time series was calculated for all transect point trends by a MK trend test. The MK test statistically assesses if there is a monotonic upward or downward trend of the variable of interest over time. The MK ranked correlation τ is calculated as

$$\tau = S/n(n-1)/2, \text{ and} \quad (5)$$

$$S = \sum_{t1}^{k-1} \sum_{t2}^{k} sgn\,[(y_{t2} - y_{t1})(x_{t2} - x_{t1})]\,,$$

where n is the sample size, k is the number of years and $t1$ and $t2$ are the years 2000 to 2016 (in this study t1=2000, t2=t1+1).The y is the phenology metric and x is the time in trend analysis. The $sgn()$ is sign indicator function, which determines the sign for all possible differences, it takes values 1, 0 and -1 according to positive, zero or negative values, respectively.

The MK test produces outputs of z-scores written as

$$Z = S - sgn(S)/\sqrt{\frac{n(n-1)(2n+5)}{18}}\,, \quad (6)$$

where n is the number of years. Z-score allows the assessment of the direction and the significance of a trend. A positive z-score ($\geq$ 1.65) is a critical value that indicates a significant increase in the VI phenology metrics, when using confidence level (α) of 95% (p-value = 0.05), a negative z-score ($\leq$ 1.65) represents a significant decrease (α = 95%, p-value = 0.05) over the time period (2000 – 2016).

4 RESULTS

4.1 Phenological characteristics variability across the study area

4.1.1 PPI and NDVI derived phenology metrics

4.1.1.1 PPI and NDVI seasonality

PPI and NDVI seasonality (Figure 4) was calculated from the PPI and NDVI values (averaged from all the transect points) over the period of interest (2000-2016). Both VIs depicted seasonal patterns of vegetation growing and non-growing periods. It can be seen that peaks in PPI and NDVI values corresponded for most years. However, a pronounced difference in PPI and NDVI curves was observed. Compared to PPI, NDVI increases rapidly earlier and decreases later in all of the observed years. NDVI time-series had fluctuations, especially in the non-growing periods, while the PPI curve is smoother and has more gradual changes in the transition periods between growing seasons.

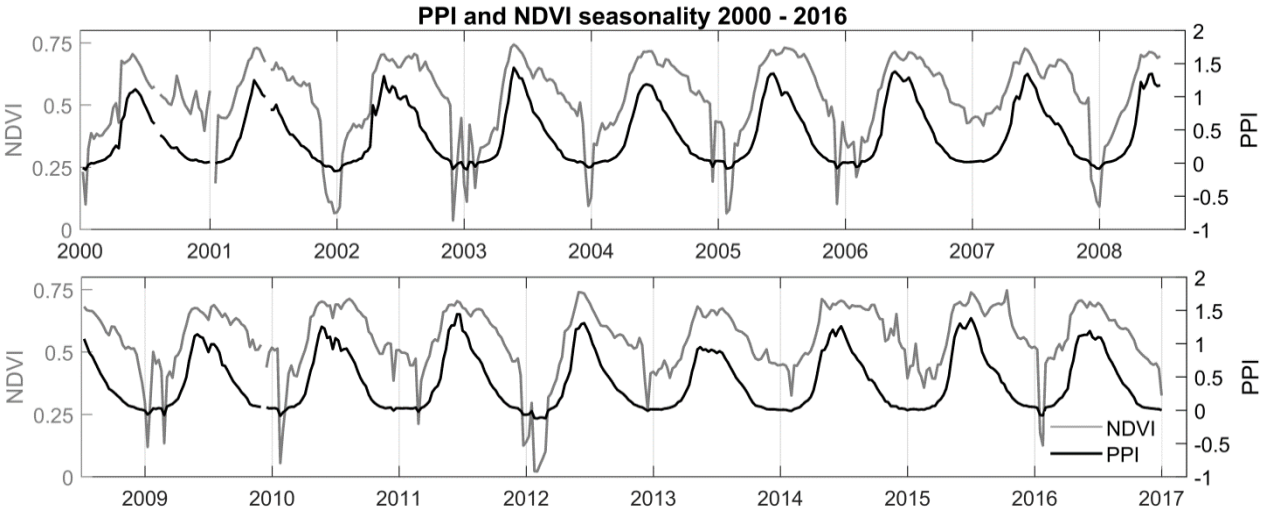

Figure 4. PPI and NDVI time-series seasonality 2000 - 2016 (pixel values from all 342 transect points were averaged for each year).

4.1.1.2 Phenology metrics

4.1.1.2.1 Start of season (SOS)

SOS derived from PPI and NDVI were averaged over 17 years (2000-2016). The mean SOS dates for both VIs were relatively close in spring time. As illustrated in Figure 5, PPI SOS estimated the beginning of the growing season to be around 20 April (DOY 108) and NDVI SOS was found to be around 18 April (DOY 106). Disparities in spatial patterns of SOS estimates were observed between the two VIs (Figure 6). The most striking characteristic was the lack of NDVI SOS observations at the highest altitudes. Earlier PPI SOS onset (before 1 April) was detected in the most southern areas (along the Mediterranean coast) as well in the lowlands, occupied mostly by agricultural vegetation. PPI SOS showed a clear elevation gradient of delayed onset towards higher altitude, indicating that the vegetation growing season starts after 10 May. The largest differences between PPI and NDVI (Figure 9A, positive values equivalent to earlier NDVI SOS), were found in the mountain regions – the Julian and Dinaric Alps, the Adriatic Mountains, the Carpathians Mountains, the Balkan Mountains etc.; where NDVI SOS was preceding PPI SOS. Areas with earlier PPI SOS dates are located close to the Adriatic and Mediterranean coast and further inland in the Pannonian plain, the Wallachian Plain and the Thracian Plain.

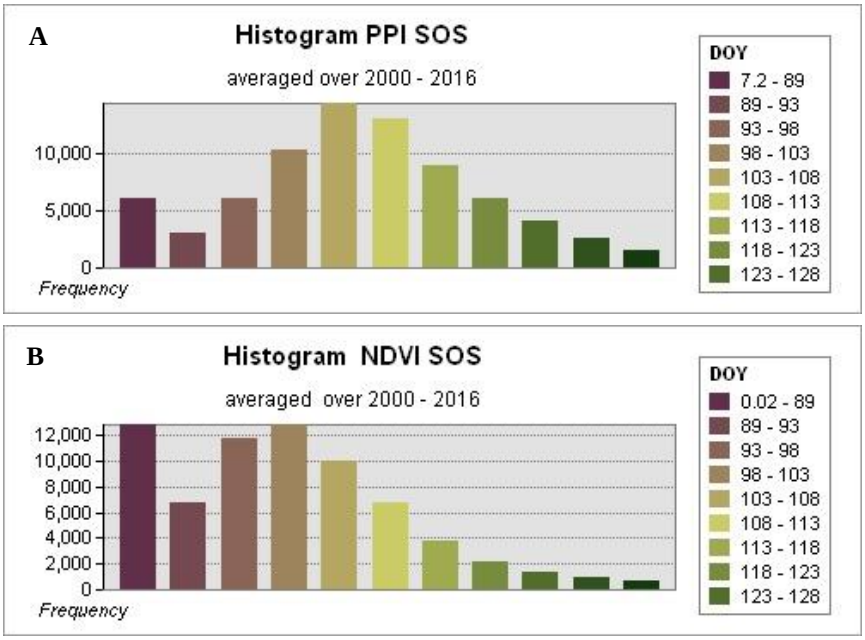

Figure 5. A) Histrogram of PPI start of season (mean – 108; standard deviation - 16); B) Histrogram of NDVI start of season (mean – 106; standard deviation - 34). Histograms were generated from raster images in maps in Figure 6.

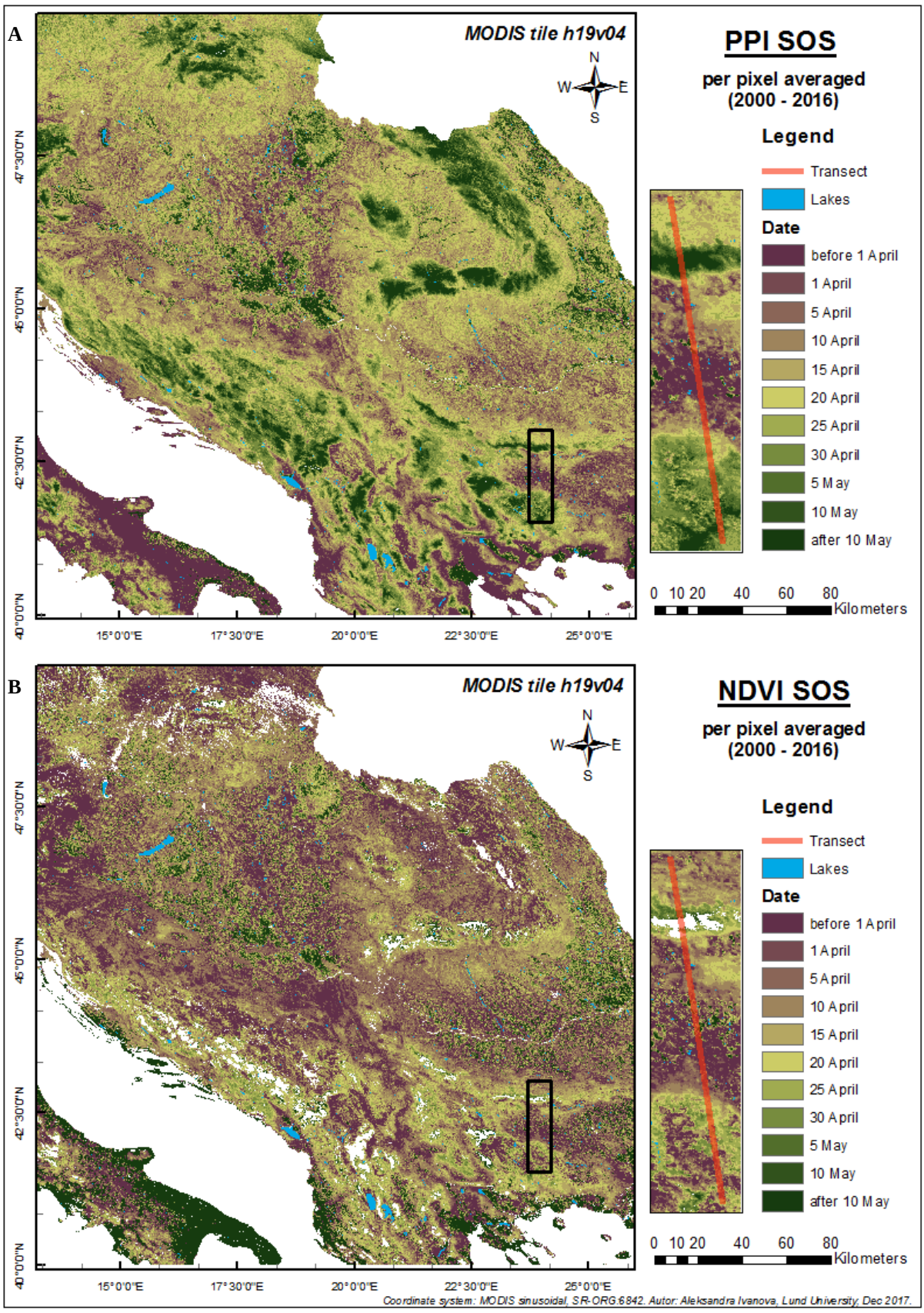

Figure 6. A) PPI start of season dates estimates averaged per pixel;

B) NDVI start of season dates estimates averaged per pixel.

4.1.1.2.2 End of season (EOS)

Similarly to SOS, averaged PPI EOS and NDVI EOS dates have an overall difference of two days (Figure 8). NDVI EOS was ending earlier in the year – around 16 September (258 DOY), whereas PPI EOS was estimated to be around 18 September (260 DOY) (Figure 7). The NDVI EOS differences from PPI (Figure 9B) were indicating that PPI EOS ended before NDVI EOS across the study area, despite the earlier averaged NDVI EOS date.

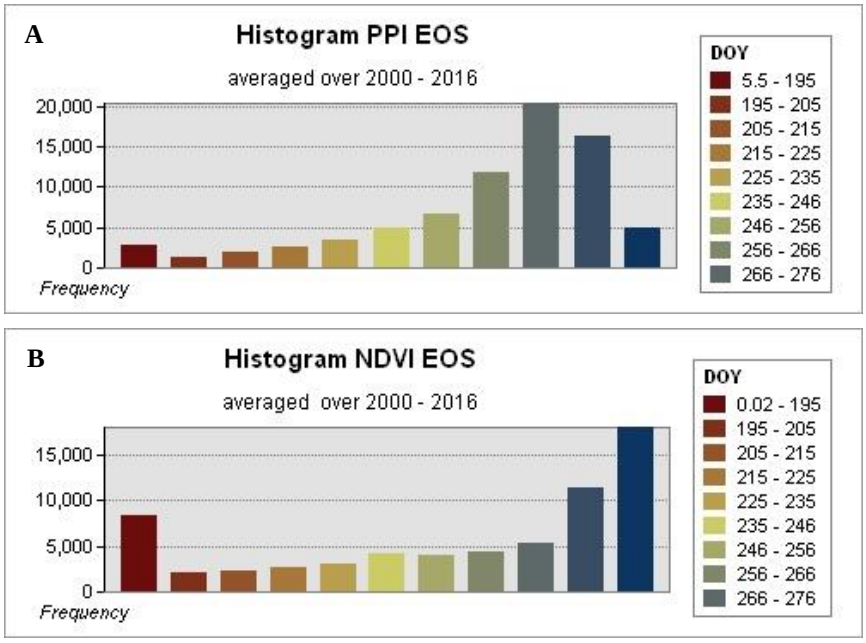

Figure 7. A) Histrogram of PPI end of season (mean – 260; standard deviation - 27); B) Histrogram of NDVI end of season (mean – 258; standard deviation - 45). Histograms were generated from raster images in maps in Figure 8.

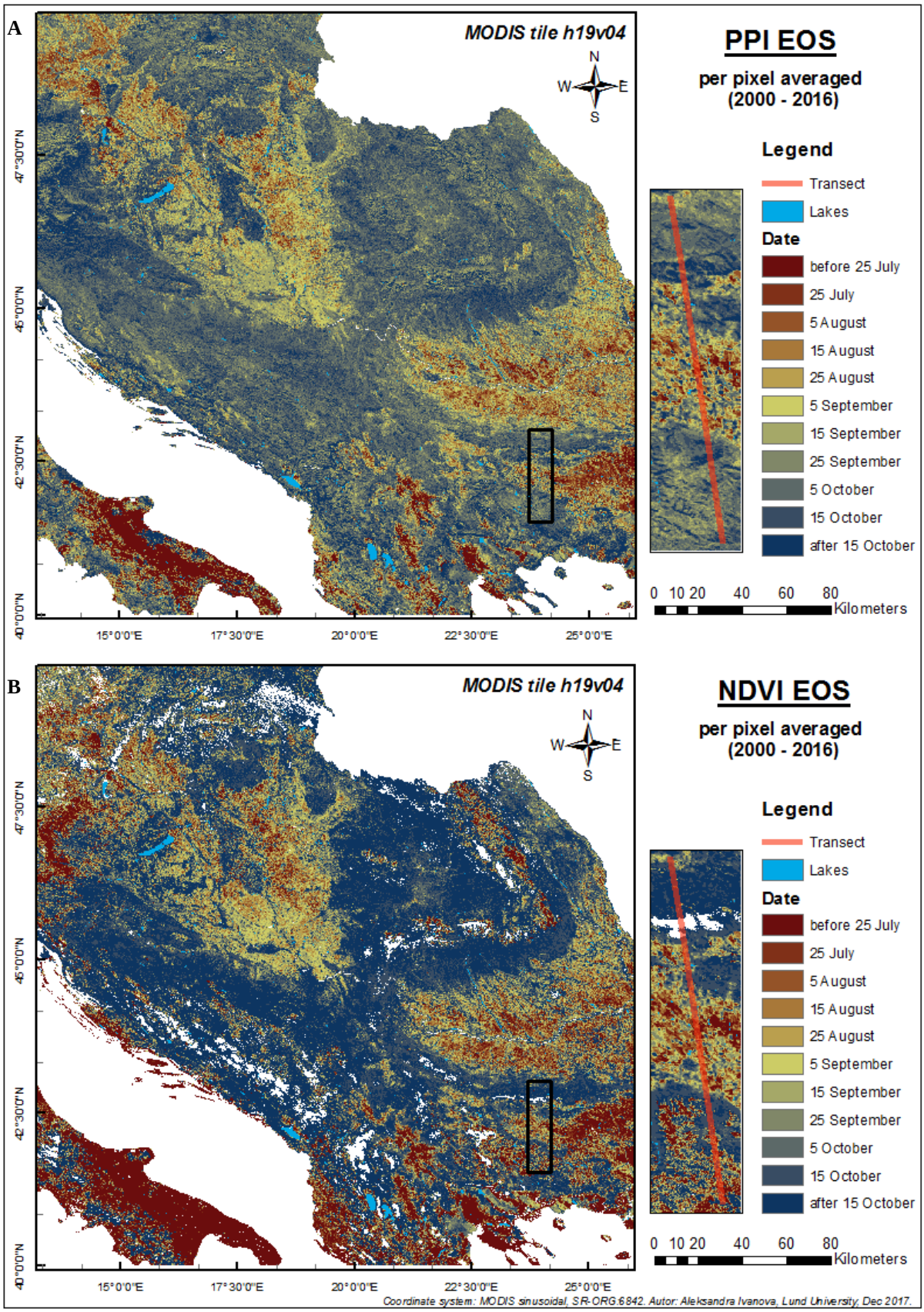

Figure 8. A) PPI end of season dates estimates averaged per pixel;
B) NDVI end of season dates estimates averaged per pixel.

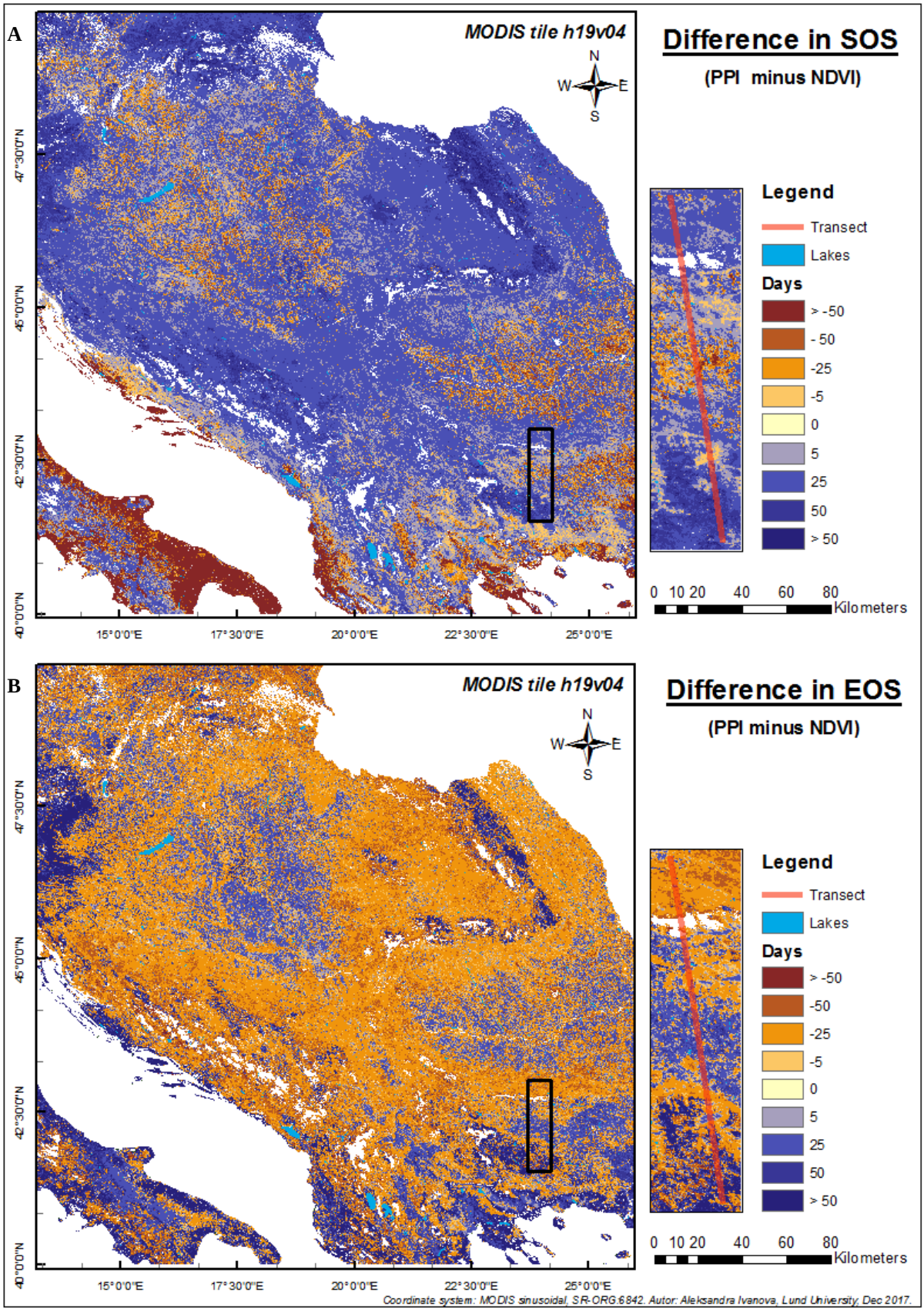

Figure 9. A) Difference in PPI and NDVI start of season;

B) Difference in PPI and NDVI end of season.

4.2 Phenological characteristics variability along transect

4.2.1 PPI and NDVI derived phenology metrics

In (Figure 10) averaged PPI and NDVI phenology metrics (± one standard deviation) are presented for each year between 2000 and 2016. The PPI mean SOS date for the whole period was around 21 April (DOY 109). Mean NDVI SOS was estimated to be earlier – 6 April (DOY 98) and preceding PPI SOS throughout the whole time period. However, both VI SOS dates follow similar temporal patterns; the latest SOS was observed in 2002 and the earliest SOS in 2016.

Averaged EOS date for PPI was approximately 21 September (DOY 262) and the NDVI EOS mean date was around 5 October (DOY 276). NDVI EOS estimates were later in the year compared to PPI EOS over the time period. It has to be noted that after year 2008, NDVI EOS mean dates were advancing with a trade-off of plummeting standard deviation values, which imply spreading of EOS phenology phase timings within the year.

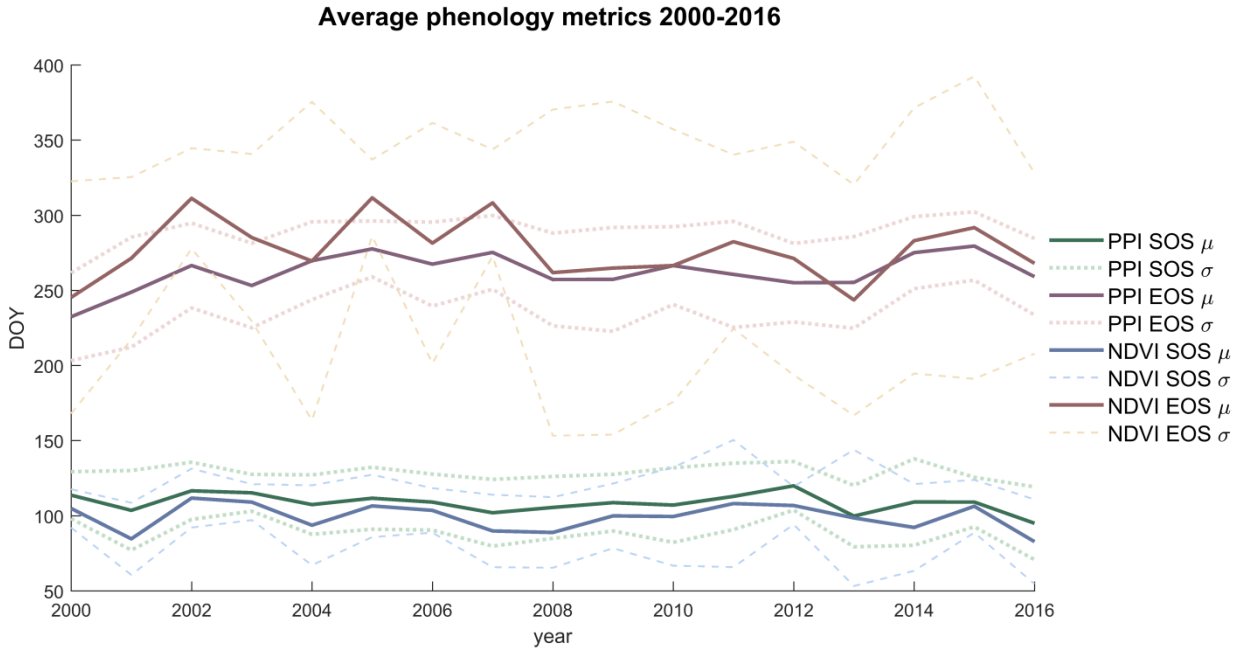

Figure 10. Averaged PPI and NDVI phenology metrics time-series 2000 to 2016 (mean DOY, ± one standard deviation).

4.2.2 Relationship between phenology metrics and climate factors

The obtained results (Figure 11), suggest that the increase in PPI SOS by one DOY (one day later in the year) was associated with a minor decline in temperature by 0.03Cº and an increase in precipitation with 0.23 mm. In contrast, NDVI SOS delay of one day was explained by an increase in temperature by 0.1Cº and a moderate increase in precipitation sum of 0.05 mm.

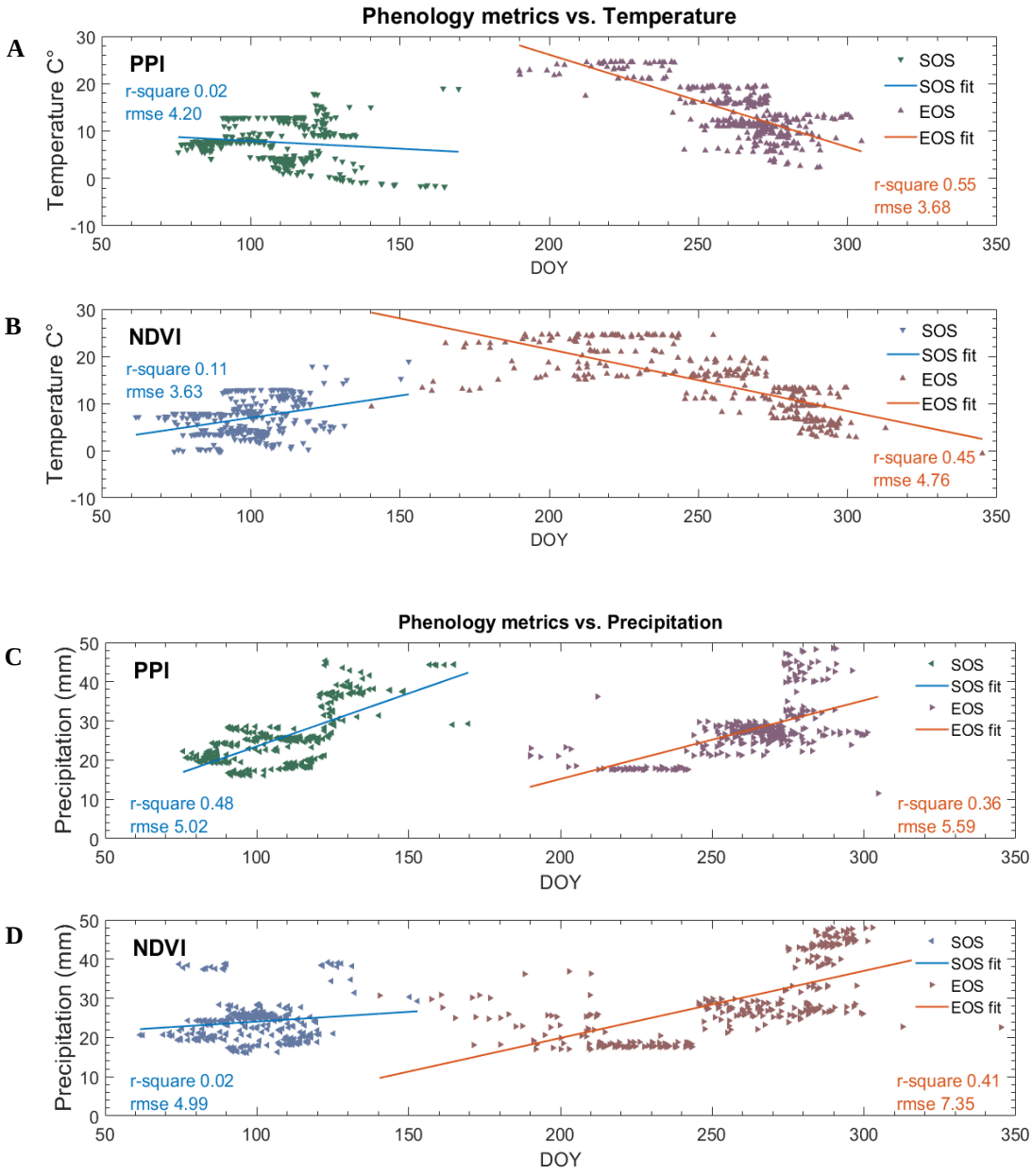

Figure 11. A) PPI start of season and PPI end of season vs. temperature;
B) NDVI start of season and NDVI end of season vs. temperature;
C) PPI start of season and PPI end of season vs. precipitation;
D) NDVI start of season and NDVI end of season vs. precipitation

PPI and NDVI estimates had negative relationship between EOS and mean temperature, (Figure 11A,B). Results showed that delay with one DOY for PPI EOS and NDVI EOS was correlated with decrease in temperature by around 0.2C° and 0.1C°, respectively. Positive correlation with precipitation for both PPI EOS and NDVI EOS was denoted, meaning that lower temperatures and higher precipitation sums promoted later EOS.

4.2.3 Relationship between phenology metrics and elevation

The relationships between VIs phenology metrics and changes in elevation are shown in Figure 12. There was a positive trend revealed for the examined phenology metrics, irrespective of index used, indicating a delay in DOY with increase in elevation. PPI SOS demonstrated strong correlation, denoting delay in onset of around 4 days with an elevation gain of 100 meters, while NDVI SOS implied change of 8 days per 100 meters. Overall the beginning of the growing season has a better correlation with elevation, with PPI SOS r-squared = 0.68 and NDVI EOS r-squared = 0.12, compared to EOS, where PPI EOS r-squared = 0.15 and NDVI EOS r-squared = 0.01.

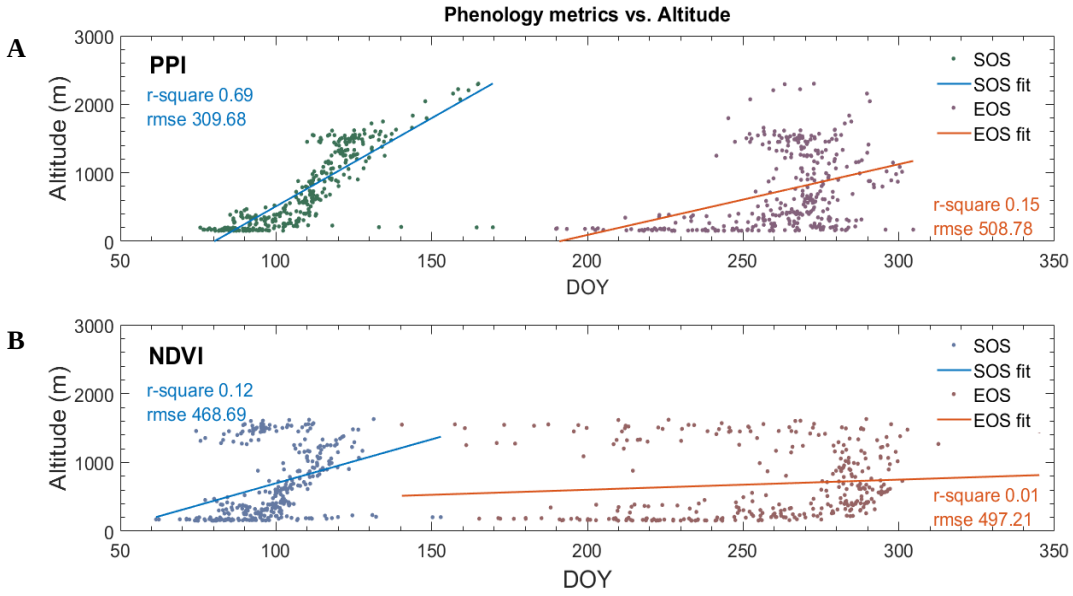

Figure 12.A) PPI start of season and PPI end of season vs. elevation;
B) NDVI start of season and NDVI end of season vs. elevation.

4.2.4 Trends in phenology metrics

The result of the Mann-Kendall trend test from the PPI and NDVI phenology metrics, for all transect points are shown in Figures 13, 14). A rather small number of observed points (< 50%) presented significant phenology trends. Nonetheless, these trends had considerable variations. Therefore, further trend analysis was conducted addressing all points, including the ones with statistically insignificant trends ($p < 0.05$).

The mean PPI derived SOS has advanced with an average rate of 0.44 days / year, EOS has delayed 0.68 days / year. Equivalently, NDVI SOS has advanced on average by 0.43 days / year, while at the same time NDVI EOS trend showed an advance in the year with 0.20 days / year.

Further, the phenology metrics trends of different land cover types were examined (Figure 15). For PPI derived phenology metrics, all land cover types showed agreement with the general trends, implying advanced SOS and respectively delayed EOS. NDVI patterns in SOS followed PPI SOS trends, except for coniferous forest. On the contrary, NDVI phenology was showing the opposite trend for EOS, suggesting change towards the earlier end of the growing season for all land cover types, except broadleaved forest.

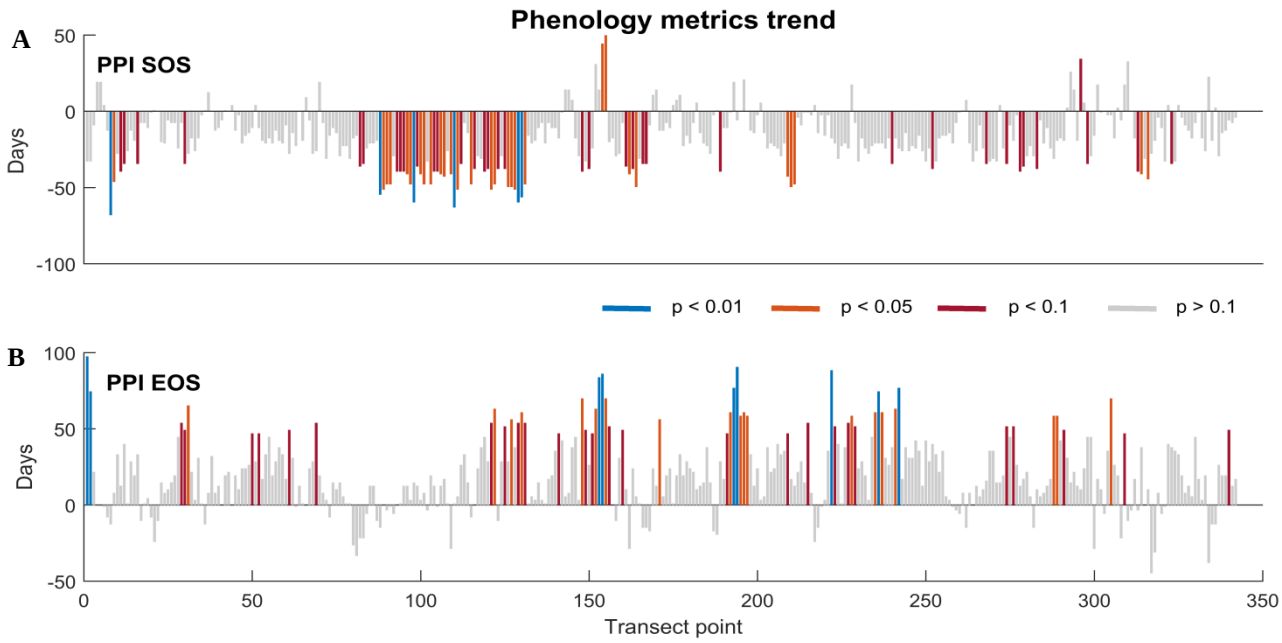

Figure 13. PPI start of season (A) and PPI end of season (B) change trends for 2000 to 2016 in days. Significance in changes at 95% confidence level: blue –strong significance (p <0.01); orange – significance (p <0.05); red - weak significance (p <0.1); grey bars - insignificant (p >= 1).

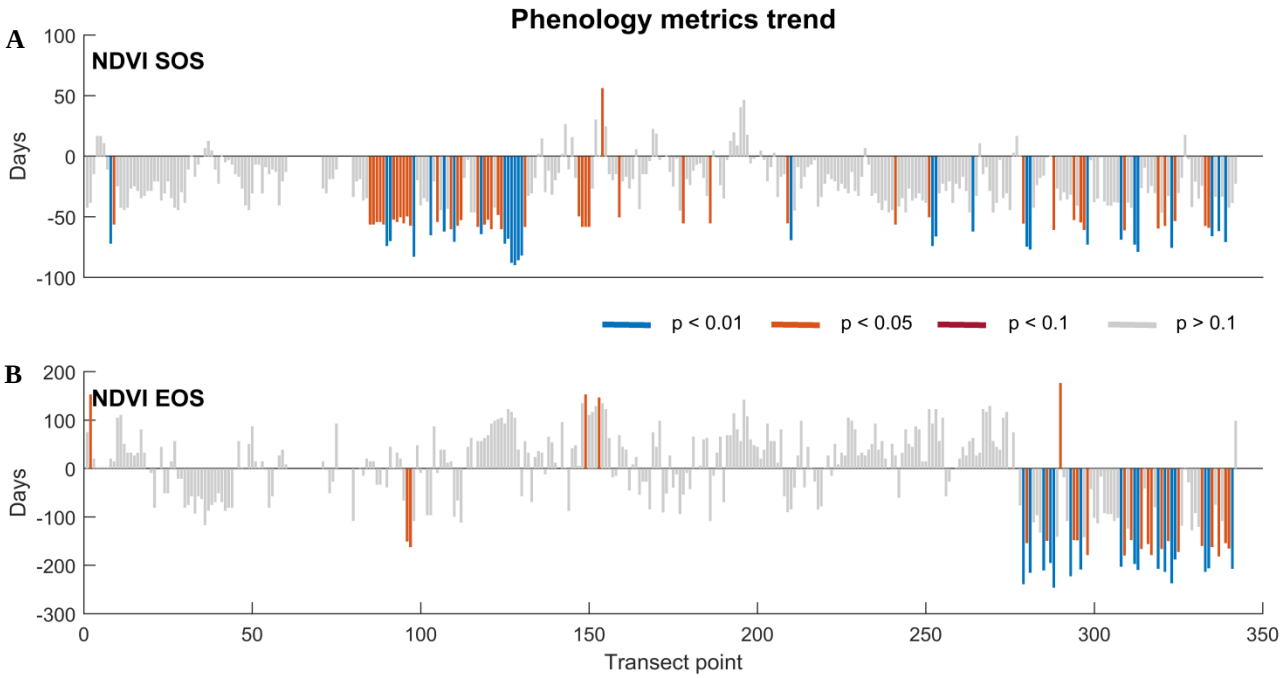

Figure 14. NDVI start of season (A) and NDVI end of season (B) change trends for 2000 to 2016 in days. Significance in changes at 95% confidence level: blue –strong significance (p <0.01); orange – significance (p <0.05); red - weak significance (p <0.1); grey bars - insignificant (p > = 1).

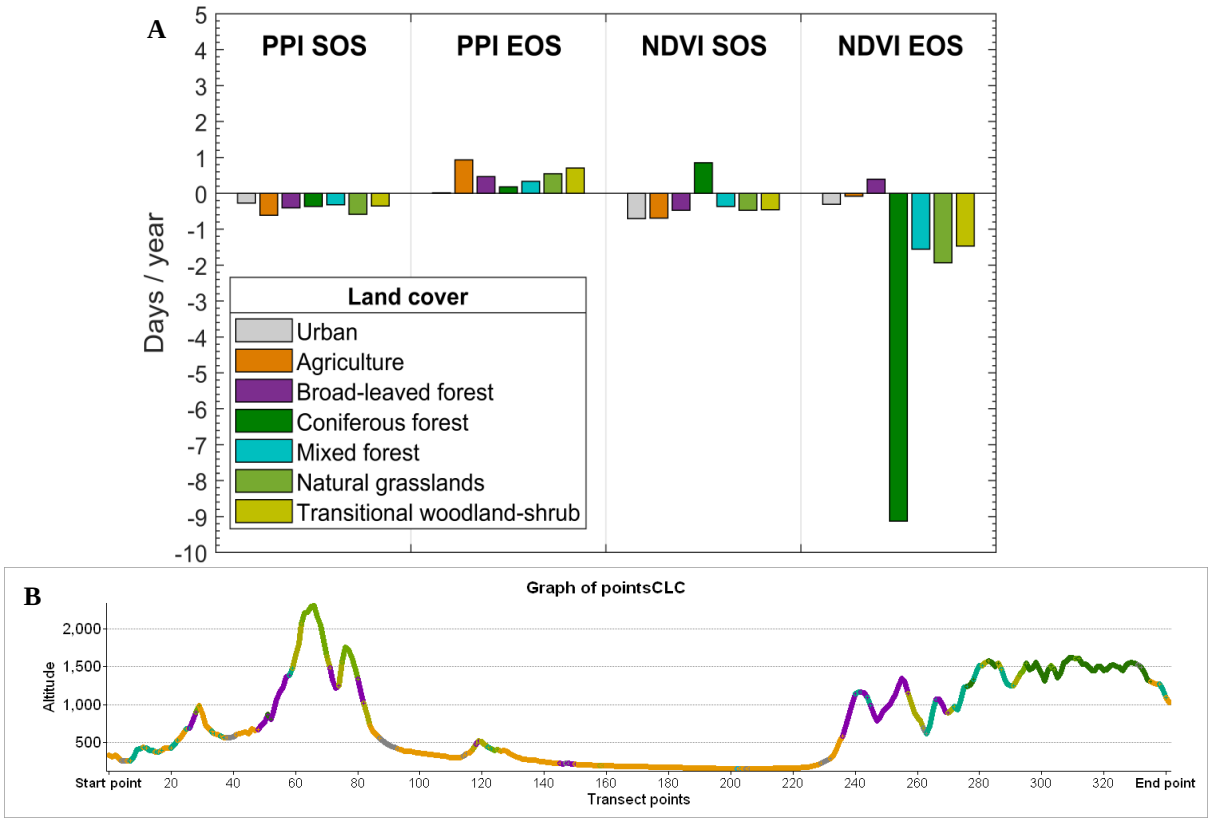

Figure 17. A) Trends (days/year) for different land cover types along the transect (according to CORINE land cover nomenclature);
B) Vertical profile of the land cover types across the transect.

4.2.5 Satellite-based phenology vs. ground phenology observations

In Table 1 VIs SOS estimates were compared with long-term date averages of growing stages of broadleaved and coniferous species from ground observations. For broadleaved forest, the results showed that the average PPI SOS date (DOY 117) was closer to "Leaf unfolding" stage timings (DOY 123), whereas NDVI SOS (DOY 112) corresponded to the stage of "First budburst" (DOY 112). The beginning of the growing season in coniferous forest was better depicted by PPI SOS (DOY 121), which corresponded to the "First budburst" observation date (DOY 123), whereas NDVI SOS (DOY 98) was close to a month earlier in the year, preceding that first growing stage of coniferous forests .

CORINE land cover types	Satellite-based phenology		Ground observation	
	PPI SOS	NDVI SOS	First budburst	Leaf unfolding
Broadleaved forest	117 ± 7	112 ± 9	112	123
Coniferous forest	121 ± 10	98 ± 18	123	145

Table 1. PPI and NDVI derived SOS dates (± one standard deviation) and ground observation dates of corresponding growth stages for broadleaved forest and coniferous forest

The results in Table 2 showed that the ending of the growing season in broadleaved forests according to PPI EOS (DOY 275) was related to growing stage "Leaf colouring" (DOY 288), while NDVI EOS (DOY 308) was closer to the "Leaf fall" stage (DOY 305). Coniferous forest autumn seasonality, according dates for "Needle fall" stage (DOY 300), was observed to have been later in the year in comparison to satellite-based phenology estimates from both VIs. However, PPI EOS (DOY 266) was closer to "Needle fall" timings than NDVI EOS (DOY 228).

CORINE land cover types	Satellite-based phenology		Ground observation	
	PPI EOS	NDVI EOS	Leaf colouring	Leaf fall / Needle fall
Broadleaved forest	275 ± 19	308± 32	288	305
Coniferous forest	266 ± 8	228 ± 113	-	300

Table 2.PPI and NDVI derived EOS dates (± one standard deviation) and ground observation dates of corresponding growth stages for broadleaved forests and coniferous forests

5 DISCUSSION

5.1 Time-series fit and phenology metrics selection

VIs are not always accurate in reflecting vegetation dynamics, mostly due to abiotic interference with the vegetation signal. Model smoothing techniques are used to reduce the non-vegetative signal in VIs time-series. The accuracy of phenology metrics retrieved from remote sensing is strongly dependent on the approach chosen to model the annual VI data. Derivative methods were reported to be an appropriate choice for estimating phenology metrics at regional and continental scales (Beck et al. 2007; Zhang et al. 2012; Wu et al. 2017). The double logistic function was used in this work for smoothing VI signal, where the SOS and EOS estimates were extracted as points of change on a fitted curve. However, more complicated methods may not be able to produce better results. One source of uncertainty in estimating phenology metrics is related to the overfitting of the VIs time-series curves, resulting in false inflection points due to sensitivity to inter-annual variations of the signal (Wu et al. 2017).

PPI and NDVI were calculated from the same satellite data, with the same quality and under the same atmospheric conditions. However, the selected settings for extraction of phenology metrics of the NDVI fitted curve, were not depicting reliable seasonality properties in the high mountains. This resulted in no SOS and EOS found for NDVI at those areas. On the contrary, PPI was found to be less sensitive to atmospheric contamination. This could be explained by PPI's clear physical formulation and the incorporation of the site specific maximum $NIR - red$ difference, accounting for variations of vegetation NIR reflectance, usually much larger than those for red reflectance (Jin and Eklundh 2014). A commonly applied approach is the use of a defined absolute or relative threshold between the minimum and the maximum values in the VI time-series. This method works well at a local scale, because it allows easy tuning of the threshold accounting for the ecosystem specific vegetation characteristics, therefore it could be more appropriate to apply on NDVI time-series for phenology metrics retrieval for mountainous areas. However, the single threshold method was not found to be suitable for larger areas, composed of various ecosystems (Jönsson and Eklundh 2004).

5.2 PPI and NDVI derived phenology metrics

Generally, NDVI-based phenology resulted in earlier SOS and later EOS, compared to PPI-based phenology, inferring that a longer growing season was depicted by NDVI phenology estimates (Figure 5, 6). These results coincide with the findings made by Jin et al (2017), evaluating the performance of PPI and NDVI derived phenology against ground phenology data and tower measured GPP – derived phenology, estimated for 24 sited in the northern Europe. They found that NDVI phenology is more related to snow cover seasonality than to phenology metrics derived from ground observations generating earlier SOS and later EOS estimates. Similar results were obtained by Karkauskaite et al. (2017) comparing PPI and NDVI estimated SOS with GPP-retrieved SOS from 81 flux tower observations for the Boreal zone of the Northern Hemisphere. Their study reported that NDVI phenology was mostly negatively biased for SOS and positively biased for EOS, suggesting earlier SOS and later EOS estimates.

The most pronounced differences found in SOS between PPI and NDVI (Figure 9), were found in the areas influenced by Mediterranean climate: PPI estimated SOS date in the early spring (Figure 6A), whereas NDVI calculated SOS to be up to three months later in the year (Figure 6B). Along the Mediterranean coast some areas are having seasonality opposite to the rest of the study area (Gordo and Sanz 2010; Zhang et al. 2012). In some of those areas, the SOS for some plant species occurs during the autumn or early winter (detected by NDVI SOS); subsequently there is a possibility to have a secondary green-up in the spring of the next year (detected by PPI SOS). On the contrary to the coast, in the mountain areas, NDVI SOS was estimated to be as much as one month earlier then PPI SOS (Figure 6).

5.3 Phenology metrics versus climate factors

The relationship between phenology phases and climate conditions was analyzed (Figure 11), resulting in moderate correlation of SOS and EOS to climate factors, in contrast with most studies conducted on PPI and NDVI. An insignificant negative relationship was found for PPI SOS and mean air temperature (Figure 11A, r-squared = 0.02), the opposite was shown for NDVI SOS with an insignificant positive relationship (Figure 11B, r-squared = 0.01), suggesting that later SOS is associated with higher temperature. Temperature and EOS had a negative relationship (PPI EOS r-squared = 0.55, NDVI EOS r-squared = 0.45), suggesting that the delay in the end of the season is not influenced by change in temperature. A general

source of uncertainty was the use of interpolated meteorological data averaged for each month. Better approach would be the use of regional climate model and examine phenological events stratified by land cover type. More reliable results to determine temperature impact on phenology, might have been achieved if growing degree days had been used as an approximate measure of growth of vegetation (Sparks and Menzel 2002). Coinciding with other studies on PPI and NDVI, focused on high latitudes ecosystems, in Southeastern Europe, precipitation was found to have a delaying effect on SOS and EOS (Figure 11C,D). It could be inferred that the precipitation regime is governing the length of the season rather than the timing of the start of it (Wang et al. 2017). However, this simple model was not capable of describing the complex dependencies between climate factors and phenology metrics because of the simultaneous influence of all climatological factors on vegetation.

5.4 Phenology metrics versus elevation

One way of improving our understanding of the seasonal dynamics of phenology is to examine phenology metrics variations along an elevation gradient, defining vegetation elevation zonation and their phenology characteristics (Noormets 2009; Ranjitkar 2013; Schuster et al. 2014). In this study, the estimated SOS and EOS showed positive relationships to an increase in elevation (Figure 12). Spring phenology has a pronounced response to change in elevation, which agrees with general accepted knowledge. Dependence on elevation was revealed by SOS estimates, especially for PPI-based phenology (r-squared = 0.68), while NDVI SOS showed a weak positive correlation (r-squared = 0.12). According to the results for EOS estimates, elevation was not that strong indicator of autumn phenology patterns (Figure 12). PPI EOS dates have a weak positive correlation with elevation (r-squared = 0.15), similarly NDVI EOS estimates denote an insignificant positive relationship (r-squared = 0.01). Limitations in outlining the relationship between NDVI-based phenology and elevation were related to the absence of metrics estimates above 1700 meters above sea level. Moreover, sensitivity to elevation depends on differences in aspect; south facing hills are exposed to more sun light, higher temperatures and the influence of the Mediterranean climate, which can lead to a difference in phenology patterns, compared to those observed on north facing hills (Defila and Clot 2001). Phenology response to elevation is very specific on plant species and their adaptation techniques to mid- and high- elevations (Vitasse et al. 2009; Guyon et al. 2011; Liu et al. 2014).

5.5 Trends in phenology metrics

The observed phenology trends, over the period 2000 to 2016, showed good agreement with previous studies on long-term phenology (Menzel et al. 2006; Zeng et al. 2011; Jin 2015; Wang et al. 2016). PPI and NDVI phenology estimates follow the same negative trend pattern on SOS (Figure 13A, 14A), implying change towards an earlier SOS in the spring. However the two VIs do not show similar results for EOS (Figure 13B, 14B), with PPI suggesting a delay and NDVI having the opposite trend, advancing the end of the season. Trend analysis for different land cover types revealed noticeable differences between both VIs (Figure 15). The most notable differences were found for "Broadleaved forest" and "Coniferous forest" land cover types. Compared to PPI, NDVI SOS showed an opposite trend for coniferous forest, suggesting a season starting later in the year. The most striking NDVI trend was the resulting patterns in EOS for evergreen species. NDVI EOS indicated advancing date by 9.13 days / year, compared to the PPI EOS trend of delaying 0.18 days / year. The only agreement with delaying PPI EOS phenology trends was observed in NDVI trends for broadleaved forests, implying that this is the one land cover class experiencing ending of its season later in the year according to NDVI phenology. The observed trend patterns, in this study, were not found to be statistically significant for most of the evaluated points, at the 95% confidence level. This could be related to outliers in the time-series, as well to the relatively short period of investigation (seventeen years) and small sample (342 transect points) (Zhang et al. 2012). A better estimation of trend significance could have been achieved by panel data analysis (Hsiao 2004).

5.6 Ground phenology against satellite-based phenology

PPI derived phenology was generally more accurate over NDVI for estimating vegetation development in the forest sites (Table 1, 2). The smallest disagreements between the two VIs were found for broadleaved forests. PPI SOS was found to be closer to the "Leaf unfolding" stage of the growing season, while NDVI SOS captured the "First budburst" changes, observed earlier in the year (Table 1). As mentioned above, NDVI SOS indicates an increase in the canopy greenness, which could be associated with a change in snow cover rather than to plant activity (Jönsson et al. 2010; Jin et al. 2017).

With respect to coniferous forest phenology, PPI-derived phenology metrics were able to detect more precise phenology phase timings, when compared to ground observations (Table

1, 2). NDVI-derived SOS and EOS were estimated to be at least a month earlier. In addition, significant deviations of NDVI SOS (± 18 days) and NDVI EOS (± 113 days) estimates were presented, suggesting that NDVI is experiencing difficulties detecting seasonality patterns in coniferous forests.

As mentioned above, the captured signal is a mixture of reflectance signatures, depending on the chlorophyll content, leaf area and the structure of the canopy and it is disturbed by background noise, due to scale inequality between individual plants and the spatial resolution of the sensors (Reed et al. 2009). In addition, ground phenology data has inherited temporal and spatial uncertainties and the growing stages dates used, were averaged for different species (Appendix, Table A2). Therefore, these methods cannot be considered reliable for satellite-based phenology validation. Despite that, it gives a general overview of vegetation seasonality patterns at broad-leaved and coniferous forests in the study area.

The results in this study coincide with the findings in other studies discussing the limitations of NDVI in evergreen forests in comparison with PPI, which was formulated to have a linear relationship with LAI (Beck et al. 2007; Jönsson et al. 2010; Jin and Eklundh 2014; Jin 2015; Karkauskaite et al. 2017).

6 CONCLUSION

This study analyses the performance of the satellite derived Plant Phenology Index (PPI) against the Normalized Difference Vegetation Index (NDVI) for estimating start of season (SOS) and end of season (EOS) of vegetation growth in part of the Balkan Peninsula, Southeastern Europe (2000 – 2016). Results revealed that PPI and NDVI differ considerably; SOS and EOS may diverge by more than one month between the two indices. The most pronounced differences were observed in the mountain regions, where NDVI SOS occurred up to 50 days earlier then PPI. Even with changing the focus of the study, to a smaller area (transect), NDVI followed the pattern of preceding PPI in SOS and delaying in EOS estimates throughout the whole period of 2000 to 2016.

Examined phenology metrics trends showed an overall advance in SOS, with a rate of change for PPI SOS of 0.44 days/year and 0.43 days/year for NDVI. In contrast, the two VIs did not correspond with respect to EOS trends, PPI showing trends towards delaying EOS by 0.68 days/year as compared to NDVI with advancing trends by 0.20 days/year. Trends analyzed for specific cover types revealed large differences between PPI and NDVI: PPI preserves its general trends of advances in SOS and delays in EOS for all land cover types. NDVI is inconsistent in change patterns, especially for the land cover classes of coniferous forests. NDVI SOS trend for coniferous forest is the only land cover type with delayed trend patterns (0.85 days/year) for spring onset. With regard to EOS trends in coniferous forests, PPI trends were found to be delaying by 0.18 days/year, whereas NDVI showed advancing in EOS to extreme magnitude of 9.13 days/year.

PPI showed better correlation with all examined phenology driving factors – air temperature, precipitation and elevation gradient than NDVI. Consequently, PPI generated better agreement with ground phenology observations at broadleaved and coniferous forest sites, as compared to NDVI.

The main conclusion of this study supports previous findings of improved and more reliable performance of PPI over NDVI for satellite-based phenology metric retrieval. NDVI derived phenology must be interpreted with caution, particularly for land cover with dense vegetation cover and high levels of biomass, such as coniferous forests.

7 REFERENCES

Ardö, J. 2017. Calculation of phenological metrics for EEA-39 derived from remote sensing, EEA/NSS/17/001 - Final Report: 1–8.

B. Mann, H., and D. R. Whitney. 1946. On a Test of Whether one of Two Random Variables is Stochastically Larger than the Other. *Annals of Mathematical Statistics* 18.

Beck, P. S. A., C. Atzberger, K. A. Høgda, B. Johansen, and A. K. Skidmore. 2006. Improved monitoring of vegetation dynamics at very high latitudes: A new method using MODIS NDVI. *Remote Sensing of Environment* 100: 321–334. doi:10.1016/j.rse.2005.10.021.

Beck, P. S. A., P. Jönsson, K. A. Høgda, S. R. Karlsen, L. Eklundh, and A. K. Skidmore. 2007. A ground-validated NDVI dataset for monitoring vegetation dynamics and mapping phenology in Fennoscandia and the Kola peninsula. *International Journal of Remote Sensing* 28: 4311–4330. doi:10.1080/01431160701241936.

Beniston, M. 2015. *Climate Variability and Extremes during the Past 100 Years*. *Statewide Agricultural Land Use Baseline 2015*. Vol. 1. doi:10.1017/CBO9781107415324.004.

de Beurs, K. M., and G. M. Henebry. 2004. Land surface phenology, climatic variation, and institutional change: Analyzing agricultural land cover change in Kazakhstan. *Remote Sensing of Environment* 89: 497–509. doi:https://doi.org/10.1016/j.rse.2003.11.006.

Bondev, I. 1991. The vegetation of Bulgaria. Map 1: 600 000 with explanatory text. St. *Kliment Ohridski University Press, Sofia* 1: 183.

Brown, R. D., and N. Petkova. 2007. Snow cover variability in Bulgarian mountainous regions , 1931 – 2000 1229: 1215–1229. doi:10.1002/joc.

Cleland, E., I. Chuine, A. Menzel, H. A Mooney, and M. Schwartz. 2007. *Shifting plant phenology in response to global change*. *Trends in ecology & evolution*. Vol. 22. doi:10.1016/j.tree.2007.04.003.

Defila, C., and B. Clot. 2001. Phytophenological trends in Switzerland. *International journal of biometeorology* 45: 203–207.

Delbart, N., L. Kergoat, T. Le Toan, J. Lhermitte, and G. Picard. 2005. Determination of phenological dates in boreal regions using normalized difference water index. *Remote Sensing of Environment* 97: 26–38. doi:10.1016/j.rse.2005.03.011.

European Environmental Agency. 1994. CORINE Land Cover. Technical Guide. *Official Publications of the European Communities*: 1–94.

Farr, T. G., P. A. Rosen, E. Caro, R. Crippen, R. Duren, S. Hensley, M. Kobrick, M. Paller, et al. 2007. The Shuttle Radar Topography Mission. *Reviews of Geophysics* 45: n/a--n/a. doi:10.1029/2005RG000183.

Gates, D. M., H. J. Keegan, J. C. Schleter, and V. R. Weidner. 1965. Spectral Properties of Plants. *Appl. Opt.* 4. OSA: 11–20. doi:10.1364/AO.4.000011.

Gitelson, A. A. 2004. Wide Dynamic Range Vegetation Index for Remote Quantification of Biophysical Characteristics of Vegetation. *Journal of Plant Physiology* 161: 165–173. doi:https://doi.org/10.1078/0176-1617-01176.

Glenn, E. P., A. R. Huete, P. L. Nagler, and S. G. Nelson. 2008. Relationship between remotely-sensed vegetation indices and plant physiological processes: what vegetation indices can and cannot tell us about the landscape. *Sensors* 8: 2136. doi:10.3390/s8042136.

Gordo, O., and J. J. Sanz. 2010. Impact of climate change on plant phenology in Mediterranean ecosystems. *Global Change Biology* 16: 1082–1106. doi:10.1111/j.1365-2486.2009.02084.x.

Graham, A. 2012. Remote sensing of vegetation principles, techniques, and applications , edited by Hamlyn G. Jones and Robin A. Vaughn. *International Journal of Remote*

Sensing 33. Taylor & Francis: 1653–1654. doi:10.1080/01431161.2011.587097.
Guyon, D., M. Guillot, Y. Vitasse, H. Cardot, O. Hagolle, S. Delzon, and J. P. Wigneron. 2011. Monitoring elevation variations in leaf phenology of deciduous broadleaf forests from SPOT/VEGETATION time-series. *Remote Sensing of Environment* 115. Elsevier Inc.: 615–627. doi:10.1016/j.rse.2010.10.006.
Henebry, G. M., and K. M. de Beurs. 2013. Remote Sensing of Land Surface Phenology: A Prospectus. In *Phenology: An Integrative Environmental Science*, ed. M. D. Schwartz, 385–411. Dordrecht: Springer Netherlands. doi:10.1007/978-94-007-6925-0_21.
Hsiao, C. 2004. Analysis of panel data. *Computers & Mathematics with Applications* 47: 1147–1148. doi:10.1016/S0898-1221(04)90099-5.
Huete, A., T. Miura, H. Yoshioka, P. Ratana, and M. Broich. 2014. *Indices of Vegetation Activity*. *Biophysical Applications of Satellite Remote Sensing*. doi:10.1007/978-90-481-3335-2.
Jin, H. 2015. *Remote sensing phenology at European northern latitudes - From ground spectral towers to satellites*.
Jin, H., and L. Eklundh. 2014. A physically based vegetation index for improved monitoring of plant phenology. *Remote Sensing of Environment* 152. Elsevier Inc.: 512–525. doi:10.1016/j.rse.2014.07.010.
Jin, H., A. M. Jönsson, K. Bolmgren, O. Langvall, and L. Eklundh. 2017. Disentangling remotely-sensed plant phenology and snow seasonality at northern Europe using MODIS and the plant phenology index. *Remote Sensing of Environment* 198. Elsevier Inc.: 203–212. doi:10.1016/j.rse.2017.06.015.
Jönsson, A. M., L. Eklundh, M. Hellström, L. Bärring, and P. Jönsson. 2010. Annual changes in MODIS vegetation indices of Swedish coniferous forests in relation to snow dynamics and tree phenology. *Remote Sensing of Environment* 114. Elsevier Inc.: 2719–2730. doi:10.1016/j.rse.2010.06.005.
Jönsson, P., and L. Eklundh. 2004. TIMESAT - A program for analyzing time-series of satellite sensor data. *Computers and Geosciences* 30: 833–845. doi:10.1016/j.cageo.2004.05.006.
Karkauskaite, P., T. Tagesson, and R. Fensholt. 2017. Evaluation of the plant phenology index (PPI), NDVI and EVI for start-of-season trend analysis of the Northern Hemisphere boreal zone. *Remote Sensing* 9. doi:10.3390/rs9050485.
Kazandjiev, V. 2014. Phenological Development As Indicator Of Meteorological Conditions Phenological Development As Indicator Of Meteorological Conditions.
Keatley, M. R., and I. L. Hudson. 2010. *Phenological Research: Methods for Environmental and Climate Change Analysis*. *Phenological research methods for environmental and climate change analysis*. doi:10.1007/978-90-481-3335-2.
Kottek, M., J. Grieser, C. Beck, B. Rudolf, and F. Rubel. 2006. World map of the Köppen-Geiger climate classification updated. *Meteorologische Zeitschrift* 15: 259–263. doi:10.1127/0941-2948/2006/0130.
Kueppers, L. M., M. Torn, J. Harte, L. Berkeley, and C. Change. 2007. Quantifying Ecosystem Feedbacks to Climate Change : Observational Needs and Priorities. *Energy*.
Letchov, G. 2012. Assessment of land surface phenology in Central Rhodopes estimated from remote sensing for 2003–2010.: 29–30.
Lieth, H., ed. 1974. *Phenology and Seasonality Modeling*. Vol. 8. Ecological Studies. Berlin, Heidelberg: Springer Berlin Heidelberg. doi:10.1007/978-3-642-51863-8.
Liu, L., L. Liu, L. Liang, A. Donnelly, I. Park, and M. D. Schwartz. 2014. Effects of elevation on spring phenological sensitivity to temperature in Tibetan Plateau grasslands. *Chinese Science Bulletin* 59: 4856–4863. doi:10.1007/s11434-014-0476-2.
Menzel, A., Ti. H. Sparks, N. Estrella, and E. Koch. 2006. European phenological response to

climate change matches the warming pattern. *Global Change Biology* 12: 1969–1976. doi:10.1111/j.1365-2486.2006.01193.x.
Morisette, J. T., A. D. Richardson, A. K. Knapp, J. I. Fisher, E. A. Graham, J. Abatzoglou, B. E. Wilson, D. D. Breshears, et al. 2009. Tracking the rhythm of the seasons in the face of global change: Phenological research in the 21 st century. *Frontiers in Ecology and the Environment* 7: 253–260. doi:10.1890/070217.
Noormets, A. 2009. *Phenology of Ecosystem Processes*. Edited by Asko Noormets. New York, NY: Springer New York. doi:10.1007/978-1-4419-0026-5.
Parmesan, C. 2006. Ecological and Evolutionary Responses to Recent Climate Change. *Annual Review of Ecology, Evolution, and Systematics* 37: 637–669. doi:10.1146/annurev.ecolsys.37.091305.110100.
Ranjitkar, S. 2013. Effect of elevation and latitude on spring phenology of Rhododendron at Kanchenjunga Conservation Area, East Nepal. *International Journal of Applied Sciences and Biotechnology* 1: 253–257.
Reed, B. C., M. D. Schwartz, and X. Xiao. 2009. Remote sensing phenology. *Phenology of Ecosystem Processes*: 231–246. doi:10.1007/978-1-4419-0026-5_10.
Richardson, A. D., T. F. Keenan, M. Migliavacca, Y. Ryu, O. Sonnentag, and M. Toomey. 2013. Climate change, phenology, and phenological control of vegetation feedbacks to the climate system. *Agricultural and Forest Meteorology* 169: 156–173. doi:https://doi.org/10.1016/j.agrformet.2012.09.012.
Rouse, J. W., R. H. Haas, J. A. Schell, and D. W. Deering. 1973. Monitoring vegetation systems in the Great Plains with ERTS. In *Proceedings of the Third ERTS Symposium*, 1:309–317.
Schaaf, C. B., F. Gao, A. H. Strahler, W. Lucht, X. Li, T. Tsang, N. C. Strugnell, X. Zhang, et al. 2002. First operational BRDF, albedo nadir reflectance products from MODIS. *Remote Sensing of Environment* 83: 135–148. doi:10.1016/S0034-4257(02)00091-3.
Schuster, C., N. Estrella, and A. Menzel. 2014. Shifting and extension of phenological periods with increasing temperature along elevational transects in southern Bavaria. *Plant Biology* 16: 332–344. doi:10.1111/plb.12071.
Schwartz, M. D. 2013. *Phenology: An Integrative Environmental Science*. Edited by Mark D. Schwartz. Vol. 39. Tasks for Vegetation Science. Dordrecht: Springer Netherlands. doi:10.1007/978-94-007-6925-0.
Sellers, P. J. 1985. Canopy reflectance, photosynthesis and transpiration. *International Journal of Remote Sensing* 6. Taylor & Francis: 1335–1372. doi:10.1080/01431168508948283.
Sen, P. K. 1968. Robustness of Some Nonparametric Procedures in Linear Models. *The Annals of Mathematical Statistics* 39: 1913–1922. doi:10.2307/2239290.
Sparks, T. H., and A. Menzel. 2002. Observed changes in seasons: An overview. *International Journal of Climatology* 22: 1715–1725. doi:10.1002/joc.821.
Studer, S., R. Stöckli, C. Appenzeller, and P. L. Vidale. 2007. A comparative study of satellite and ground-based phenology. *International Journal of Biometeorology* 51: 405–414. doi:10.1007/s00484-006-0080-5.
Tan, B., J. T. Morisette, R. E. Wolfe, F. Gao, G. A. Ederer, J. Nightingale, and J. A. Pedelty. 2011. An Enhanced TIMESAT Algorithm for Estimating Vegetation Phenology Metrics From MODIS Data. *IEEE Journal of Selected Topics in Applied Earth Observations and Remote Sensing* 4: 361–371. doi:10.1109/JSTARS.2010.2075916.
Theil, H. 1950. A rank-invariant method of linear and polynomial regression analysis I. *Nederlandse Akademie Wetenchappen* 53: 386–392. doi:10.1007/978-94-011-2546-8.
Vitasse, Y., S. Delzon, C. C. Bresson, R. Michalet, and A. Kremer. 2009. Altitudinal differentiation in growth and phenology among populations of temperate-zone tree

species growing in a common garden. *Canadian Journal of Forest Research* 39: 1259–1269. doi:10.1139/X09-054.

Wang, S., B. Yang, Q. Yang, L. Lu, X. Wang, and Y. Peng. 2016. Temporal Trends and Spatial Variability of Vegetation Phenology over the Northern Hemisphere during 1982-2012. Edited by Shijo Joseph. *PLOS ONE* 11: e0157134. doi:10.1371/journal.pone.0157134.

Wang, X., Q. Gao, C. Wang, and M. Yu. 2017. Spatiotemporal patterns of vegetation phenology change and relationships with climate in the two transects of East China. *Global Ecology and Conservation* 10. Elsevier B. V.: 206–219. doi:10.1016/j.gecco.2017.01.010.

White, M. A., P. E. Thornton, and S. W. Running. 1997. A continental phenology model for monitoring vegetation responses to interannual climatic variability. *Global Biogeochemical Cycles* 11: 217–234. doi:10.1029/97GB00330.

van Wijk, M. T., and M. Williams. 2005. OPTICAL INSTRUMENTS FOR MEASURING LEAF AREA INDEX IN LOW VEGETATION: APPLICATION IN ARCTIC ECOSYSTEMS. *Ecological Applications* 15. Ecological Society of America: 1462–1470. doi:10.1890/03-5354.

Wu, C., D. Peng, K. Soudani, L. Siebicke, C. M. Gough, M. A. Arain, G. Bohrer, P. M. Lafleur, et al. 2017. Land surface phenology derived from normalized difference vegetation index (NDVI) at global FLUXNET sites. *Agricultural and Forest Meteorology* 233. Elsevier B.V.: 171–182. doi:10.1016/j.agrformet.2016.11.193.

Xue, J., and B. Su. 2017. Significant remote sensing vegetation indices: A review of developments and applications. *Journal of Sensors* 2017. doi:10.1155/2017/1353691.

Yurukov, S., and P. Zhelev. 2001. The Woody Flora of Bulgaria: A Review. *Schweizerische Zeitschrift fur Forstwesen* 152: 52–60. doi:10.3188/szf.2001.0052.

Zeng, H., G. Jia, and H. Epstein. 2011. Recent changes in phenology over the northern high latitudes detected from multi-satellite data. *Environmental Research Letters* 6. doi:10.1088/1748-9326/6/4/045508.

Zhang, X., M. Friedl, B. Tan, M. Goldberg, and Y. Yu. 2012. Long-Term Detection of Global Vegetation Phenology from Satellite Instruments. *Phenology and Climate Change*: 297–320. doi:10.5772/39197.

8 APPENDICES

Additional information on the data provided by NHIM-BAN is provided in the appendix tables. For meteorological stations location, meteorological observations frequency can be found in Table A1. General information on witch meteorological stations provide phenology observations for different plant species is provided in Table A2. In tables – A3, A4, A5 and A6, describe the ground phenology observation dates for different phenology phases for each plant species of interest.

Table A1. Ground meteorological stations – name, approximate location, elevation, data temporal availability and observation rate.

Station name	Location (approx.)	Elevation (m.a.s.l.)	Temporal availability	Observations rate
Botev	42.717397 N 24.917243 E	2376	2006-2015	10 days
Karlovo	42.641305 N 24.784840 E	450	2006-2010 (2011-close station)	10 days (2011 - monthly)
Plovdiv	42.137399 N 24.741797 E	160	2006-2015	10 days
Asenovrad	42.010162 N 24.864157 E	270	2006-2015	10 days
Rozhen	41.694931 N 24.738884 E	1759	2006-2015	10 days
Smolyan	41.572281 N 24.715470 E	1000	2006-2015	monthly (only temperature)

Table A2. Ground phenology observation data, organized by CORINE land cover type with associated representative species and theit temporal ans spatial availability.

Land cover type	Plant species	Temporal availability (gap years)	Station name
Coniferous forest	Spruce, Pine, Fir	1986 – 2006 (1989,1990,1992,1993,1994,1995)	Karlovo, Plovdiv, Asenovgrad, Smolyan
Deciduous forest	Oak	1987, 1988, 1991	Smolyan

Table A3. Ground phenology observations on spruce (Picea spp.) growth phases dates (DOY)

Year	Station	First buds	Needle budburst	Needle	Colored needle	Needle fall
1986	Karlovo	102	120	144		
	Plovdiv	127	135	147		
	Asenovgrad	110	130	147		
	Smolyan	133	133	154	295	
1987	Plovdiv	77	89	162	314	
	Smolyan	141	154	163	294	
1988	Karlovo	114	61	144		
	Plovdiv	133	137	145	298	
	Asenovgrad	124	137		344	
	Smolyan	125	144	163	288	
1991	Plovdiv	128	134	158	298	
	Smolyan	120	136	150	298	
1996	Asenovgrad	65	143	165	284	
1997	Asenovgrad	122	137	158	288	
1998	Asenovgrad	111	124	149	282	
1999	Asenovgrad	107	64	134	291	
2000	Karlovo		114	139		
	Asenovgrad	103	117	130	270	312
2001	Karlovo		70	115		
	Asenovgrad	108	151	155		326
2002	Karlovo	68	119	142		
	Asenovgrad	101	134	148		
2003	Karlovo	99	117	137		
	Asenovgrad	100	132	153	286	304
2004	Karlovo	89	117	142	309	286
	Asenovgrad	99	123	151	284	272
2005	Karlovo	87	118	136	258	303
	Asenovgrad	102	119	138	286	308
2006	Asenovgrad	104	117	151	272	304

Table A4. Ground phenology observations on pine (Pinus spp.) growth phases dates (DOY)

Year	Station	First buds	Needle budburst	Needle	Colored needle	Needle fall
1986	Karlovo	94	111	163	319	96
	Asenovgrad	107	127	134		
	Smolyan	101	139	142	295	101
1987	Asenovgrad	114	137	168		
	Smolyan	129	138	157	297	114
1988	Karlovo	98	119	163	323	100
	Asenovgrad	124	144	161	331	
1991	Plovdiv	128	136	148	303	
1996	Karlovo	123	137	147		
	Asenovgrad	126	135	165	286	
1997	Asenovgrad	114	130			
1998	Karlovo	117	135	148		
	Asenovgrad	111	119			
2000	Karlovo	83	102	118		
	Asenovgrad	103	117	130	270	296
2001	Karlovo	97	111	120	280	
	Asenovgrad	108	151	159	283	
2002	Karlovo	40	127			
	Asenovgrad	101	140	154		
2003	Karlovo	95	109	135	289	
	Asenovgrad	107	132	153	300	120
2004	Karlovo	90	111	133	302	
	Asenovgrad	97	123	132	288	
2005	Asenovgrad	108	119	138	284	
2006	Karlovo	79	104	135	319	
	Asenovgrad	104	117	135	268	304

Table A5. Ground phenology observations on fir (Abies spp.)
growth phases dates (DOY)

Year	Station	First buds	Needle budburst	Needle	Colored needle	Needle fall
1986	Plovdiv	127	135	147	298	304
	Asenovgrad	107	127	144		
1987	Plovdiv	138	150	162	304	314
	Asenovgrad	114	137	155	287	318
1988	Plovdiv	133	137	145	283	298
	Asenovgrad	124	134		283	328
1991	Plovdiv	128	134	150	293	298
1996	Asenovgrad	122	135	147	262	
1999	Asenovgrad	103	125	140	279	
	Karlovo	101	111	135	263	
2000	Asenovgrad	103	123	137	283	312
2001	Asenovgrad	106	117	135		316
2002	Asenovgrad	101	147	131		
2003	Karlovo	99	111	121	258	268
2004	Asenovgrad	97	123	151	293	281

Table A6. Ground phenology observations on oak (Quercus spp.)
growth phases dates (DOY)

Year	Station	First buds	Bud burst	Leaf unfolding	Flowering	Fruits	Fruit fall	Leaf coloring	Leaf fall
1987	Rozhen	218	118	136	144		269	272	299
	Smolyan	99	118	128	138	283	319	304	319
1988	Rozhen	98	108	116	133			295	300
	Smolyan	100	112	120	146	251	273	280	297
1991	Smolyan	93	108	117				289	311